universität wien

MASTERARBEIT / MASTER'S THESIS

Titel / Title

Exploring the Phytochemistry of *Faramea tamberlikiana* Müll.Arg. (Rubiaceae): Dominance of Phenylpropanoid Derivatives and Their Ecological Roles

verfasst von / submitted by

Celeste Jackson

angestrebter akademischer / in partial fulfilment of the requirements for the degree of

Master of Science (MSc)

Wien / Vienna 2024

Studienkennzahl lt. Studienblatt / degree program code as it appears on the student record sheet:	UA 066832
Studienrichtung lt. Studienblatt / degree program as it appears on the student record sheet:	Masterstudium Botany
Betreut von / Supervisor:	ao. Univ.-Prof. i.R. Dr. Karin Valant-Vetschera
Mitbetreut von / Co-Supervisor:	Mag. Dr. Johann Schinnerl

Table of Contents

List of Figures

List of Tables

Abstract

This study investigated the phytochemical composition of the *Faramea tamberlikiana* Müll.Arg., a neotropical species in the *Rubiaceae* family, and focused on determining the compound classes of potential chemotaxonomic relevance. While *Rubiaceae* is generally better known for alkaloid and iridoid biosynthesis, *Faramea* species are unique for the prominence of phenylpropanoids and iridoids. In *F. tamberlikiana*, three major phenylpropanoids: hydroxychavicol, and the two eugenol derivatives 2-methoxy-4-(2-propen-1-yl)phenyl-6-*O*-D-apio-β-D-furanosyl-β-D-glucopyranoside, and ligusinenoside A, dominate the chemical profile. Additionally, two terpenoids, blumenol C glucoside and deacetylasperulosidic acid, were identified. Trace amounts of tectoridin, an isoflavonoid, and vanillic acid, a phenolic acid derivative, were also isolated. These compounds play critical ecological roles, ranging from herbivory defense to symbiote signalling.

This research aimed to characterize the specific phytochemical profile of *Faramea tamberlikiana* and assess the ecological significance of the identified compounds. The study tested two eugenol derivatives isolated from this species, along with commercially available eugenol, in antifeedant assays against *Spodoptera littoralis* (Noctuidae). The insect repellent effects of these substances were clearly demonstrated. Overall, the findings show that *F. tamberlikiana* holds a unique position among Rubiaceae species studied to date due to its accumulation of phenylpropanoid derivatives, highlighting the importance of these compounds not only as fragrances but also as agents in chemical defense.

Zusammenfassung

In dieser Arbeit wurde die phytochemische Zusammensetzung von *Faramea tamberlikiana* Müll.Arg., einer neotropischen Art aus der Familie der Rötegewächse (Rubiaceae), untersucht. Die Arbeit konzentrierte sich darauf, die für den Verwandtschaftskreis um *Faramaea* typischen Verbindungsklassen der speziellen Metabolite zu identifizieren. Während diese Pflanzenfamilie im Allgemeinen besser für die Biosynthese von Alkaloiden und Iridoiden bekannt ist, weichen Arten der Gattung *Faramea* durch das Vorkommen von Phenylpropan-Derivaten und Iridoiden davon ab. In der untersuchten Art *F. tamberlikiana* dominieren im Wesentlichen die drei Phenylpropanoid-Derivat das chemische Profil: Hydroxychavicol, und die beiden Eugenol-Derivate 2-Methoxy-4-(2-propen-1-yl)phenyl-6-*O*-D-apio-β-D-furanosyl-β-D-glucopyranosid und Ligusinenosid A. Zusätzlich wurden das Megastigman-Derivat Blumenol C Glucosid und das Iridoid Deacetylasperulosidinsäure, identifiziert. Spuren von Tectoridin, einem Isoflavonoid, und Vanillinsäure, einem Derivat der Phenolsäuren, wurden ebenfalls identifiziert. Alle diese Substanzen wurden isoliert und deren Identität mithilfe von Kernresonanzspektroskopie (NMR) und Massenspektrometrie (MS) aufgeklärt. Von den beiden identifizierten Eugenol-Derivaten sowie auch vom käuflich erworbenen Eugenol selbst wurden deren frasshemmende Wirkung gegenüber Raupen der tropisch/subtropisch verbreiteten Insektenart *Spodoptera littoralis* Boisduval. getestet. Dabei zeigten sich eindeutig die insektenabwehrende Wirkung dieser Substanzen. Die Ergebnisse dieser Arbeit zeigen klar, dass *F. tamberlikiana* durch die Akkumulation von Phenylpropan-Derivaten eine Sonderstellung innerhalb bisher untersuchen Arten dieser Pflanzengruppe einnimmt und weiters, dass Phenylpropan-Derivate nicht nur als Duftstoffe, sondern auch in der chemischen Verteidigung eine wichtige Rolle einnehmen.

Acknowledgements

I would like to thank my supervisor, Dr. Karin Vetschera, for her guidance, especially during the writing of this thesis. The feedback she provided improved my paper greatly and helped me create a document I am proud of. I am also deeply grateful to my co-supervisor, Dr. Johann Schinnerl, whose mentorship was pivotal to my lab experience and to the success of this research. His expertise in extraction techniques provided the foundation for much of the work presented here, and his constructive edits contributed significantly to the clarity and rigor of this thesis. Thanks also to Dr. Andreas Berger for letting me use his photos of *Faramea tamberlikiana* and ongoing support throughout the project. I am also grateful to Milica Grubac for her assistance in isolating compounds in the water phase, which were particularly tricky to purify.

Lastly, I would like to thank my parents, Mike and Jeanne Jackson, for their unwavering support and encouragement throughout my studies, with a special thanks to my dad for his meticulous eye in double-checking my typos. My heartfelt thanks also go to my partner, Thomas, whose steadfast support has been invaluable throughout this journey. A special thank you to Andrea Pokorny for her constant encouragement, kindness, and support, which she so generously provided whenever I needed it.

1.0 Introduction

Faramea tamberlikiana Müll.Arg. (Figure 1) belongs to the *Rubiaceae* family, one of the largest plant families, renowned for its diverse genera rich in ecologically and pharmacologically significant chemical compounds (see also 1.1.1 Family: *Rubiaceae*, Stevens, 2017). The species falls within the *Rubioideae* subfamily, the largest in *Rubiaceae*, characterized by the presence of raphides in leaf tissues and major clades of herbaceous plants (see further 1.1.2 Subfamily: *Rubioideae*, Thureborn et al., 2022). *Faramea* is part of the *Coussareeae* tribe, which is notoriously difficult to classify due to significant morphological variability and cryptic species, which often necessitates DNA sequencing for accurate identification (see chapter 1.1.3 Tribe: *Coussareeae*, Löfstrand et al., 2019). The genus *Faramea*, comprising around 170 species of woody plants from shrubs to medium-sized trees, is distributed from Central Mexico to Paraguay, and shows high diversity in the Atlantic Forest of Brazil (Löfstrand et al., 2021). Its wide-ranging and variable morphological traits complicate traditional taxonomy, suggesting that chemotaxonomic markers may offer better tools for classification (see section 1.1.4 Genus: *Faramea*).

In *Rubiaceae*, phytochemical markers have long been a tool for further organization and taxonomic classification (see also 1.2.5 Phytochemistry of *Rubiaceae*). Different subfamilies, such as *Ixoroideae*, *Cinchonoideae*, and *Rubioideae*, are characterized by distinct chemical profiles, with Rubioideae being the most chemically diverse (Martins and Nunez, 2015). Within this phylogenetic context, the genus *Faramea* is notably active in biosynthesizing two primary classes of compounds: phenylpropanoids and iridoids (see section 1.2.6 Phytochemistry of *Faramea* Species), which play key roles in plant defense and interactions with the environment. Phytochemically, previous reports indicated primarily iridoids, flavonoids and anthraquinones as major constituents in *Faramea* species (Table 1). The main iridoids identified include deacetylasperulosidic acid and monotropein, while phenolic compounds, such as flavanones, flavanols, and flavanol glycosides are widely distributed across species (Barboza et al., 2018; Wolff et al., 2019; Sauvain et al., 1994). These compounds are integral to plant-environment interactions that contribute to survival and adaptability;

they function as defense mechanisms against herbivores and pathogens, or as attractants to pollinators or dispersers (see further 1.2.2.1 Iridoids and 1.2.4 Phenolics and Polyphenolics).

This phytochemical study focuses on the neotropical *Faramea tamberlikiana* and aims to identify the dominant compounds in the species. Based on these data, along with a literature review of the genus as a whole, their potential chemotaxonomic significance will be explored. Furthermore, the anti-herbivory properties of the major isolated compounds will be investigated using the larvae of the generalist *Spodoptera littoralis* (Noctuidae) to assess the ecological significance of these metabolites. By characterizing the phytochemical profile of *F. tamberlikiana*, this research aims to enhance our understanding of the roles these compounds play in the plant's ecological interactions, including their potential defensive mechanisms against herbivores and their contributions to plant fitness in diverse environments.

Figure 1: *Faramea tamberlikiana* subsp. *sessifolia*, taken by Dr. Andreas Berger in La Gamba Field Research station, Costa Rica in 2016.

1.1 Systematics

1.1.1 Family: *Rubiaceae*

The *Rubiaceae* family, also known as the coffee family, is a diverse group of flowering plants comprising around 13,465 species across 611 genera. It is one of the most significant families of flowering plants, and encompasses herbs, shrubs, and trees. *Rubiaceae* species are found in nearly every region of the world but are predominantly concentrated in tropical and subtropical regions. This family is characterized by its distinctive opposite or whorled leaves, interpetiolar stipules, and tubular, actinomorphic flowers with an inferior ovary (Stevens, 2017). Many well-known plants belong to the *Rubiaceae* family, including coffee (*Coffea* L.) and gardenias (*Gardenia* J. Ellis).

1.1.2 Subfamily: *Rubioideae*

Traditionally, the large *Rubiaceae* family has been classified into several subfamilies. While the phylogenetic relationships within *Rubiaceae* remain incompletely resolved and occasionally contentious, the family has historically been divided into three major subfamilies: *Cinchonoideae* Raf., *Ixoroideae* Raf., and *Rubioideae* Juss. (Bremer et al., 1995). In the past, these subfamilies were delineated based on molecular sequencing data, as well as on prior morphological and anatomical analyses. However, more recent extensive data analyses suggest a potential integration of the *Cinchonoideae* and *Ixoroideae* subfamilies, indicating that this issue remains unresolved (Robbrecht and Manen, 2006).

Faramea Aubl. belongs to *Rubioideae*, the largest subfamily, which contains over 8,000 species, or nearly sixty percent of *Rubiaceae* as a whole. This makes *Rubioideae* highly diverse, but several key morphological traits are shared among species, including raphides, or needle-shaped crystals of calcium oxalate, in leaf tissues, valvate corolla aestivation, indumentum of septate hairs, and heterostyly. While *Rubiaceae* is mainly comprised of woody shrubs and trees, *Rubioideae* is the only subfamily that contains major clades of herbaceous plants. Additionally, *Rubioideae*

deviates from the traditional *Rubiaceae* members in that some groups are distributed to temperate, rather than tropical or subtropical, regions (Thureborn et al., 2022).

Within *Rubioideae*, there are two major alliances (Figure 2): the pantropical *Psychotrieae* L. alliance and the cosmopolitan *Spermacoceae* L. alliance, each of which contains over 3,000 species. These two alliances account for nine and thirteen, respectively, of the twenty-nine tribes within *Rubioideae*. A third, albeit much smaller, major group of early-diverging lineages is the *Coussareeae* Hook.f. tribe. The phylogeny is not completely resolved, but it is suggested that the divergence events that separated the three lineages *Coussareeae*, *Spermacoceae*, and *Psychotrieae* occurred within a short time frame, leading to extensive incomplete lineage sorting. It is therefore difficult to assess whether *Coussareeae* is sister to the *Spermacoceae* alliance or sister to a clade comprising both, the *Spermacoceae* alliance and the *Psychotrieae* alliance (Thureborn et al., 2022).

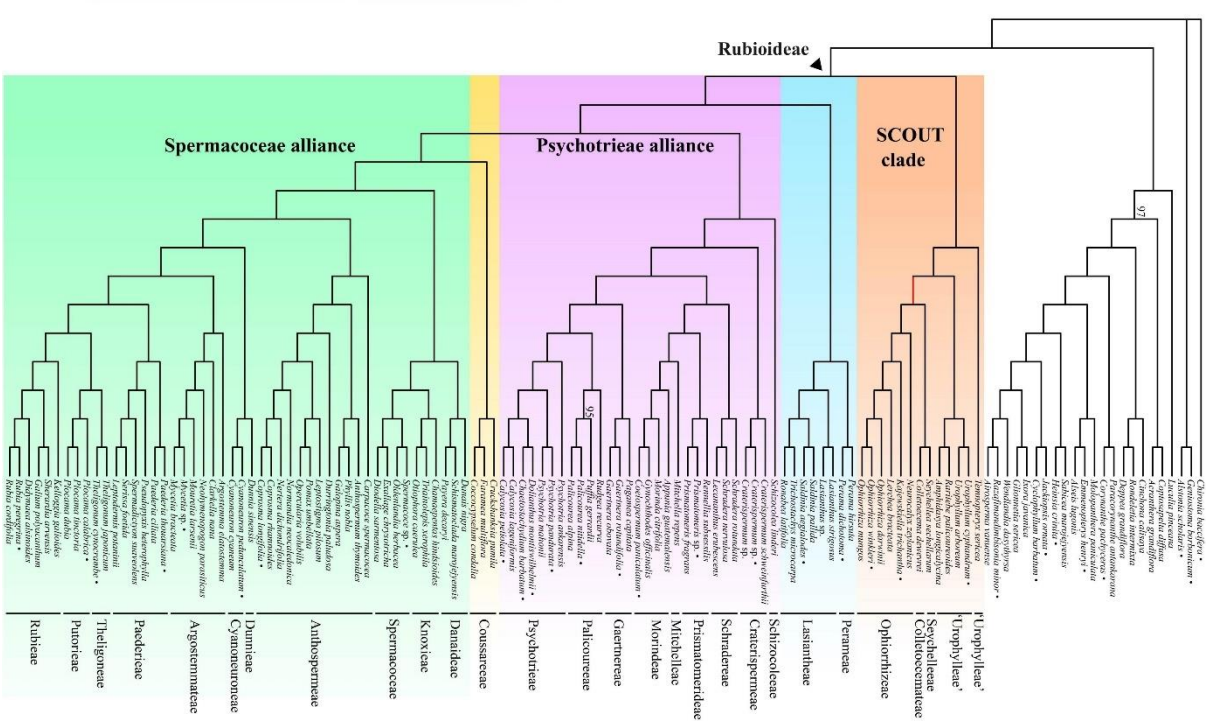

Figure 2: One proposed phylogenetic tree for the subfamily *Rubioideae* regarding *Coussareeae* tribe divergence. Concatenation-based tree estimated using IQ-TREE, 101 *Rubioideae* species sampled. Modified from Thureborn et al., 2022.

1.1.3 Tribe: *Coussareeae*

The tribe *Coussareeae* is a morphologically heterogeneous group of 330 neotropical species spanning 10 genera. Because of the variable morphology of these species, this tribe was not identified until relatively recently, when molecular data revealed their shared ancestral history. In fact, many members were placed far apart on phylogenetic trees because of their lack of visual similarities. The growth habits of plants in this tribe can be very different, from herbaceous plants to shrubs and even trees. Within this tribe, the inflorescences observed are highly variable, even within genera, and their flowers can range from showy to inconspicuous; corollas can be blue, white, or yellow. The inflorescences are typically variations of cymes, or floral clusters in which the central flower opens first and are often showy. Additionally, the fruit types are wide ranging and highly varied. This broad character diversification accounts for the ongoing conflicts in taxonomic placements (Löfstrand et al., 2019).

In recent years, there has been an effort to relate molecular systematic data with morphological character studies in order to identify potential synapomorphic features. Figure 3 presents the phylogenetic tree sorted into three suprageneric clades: *Coussarea-Faramea*, *Cruckshanksia* Hook. & Arn., and *Coccocypselum* P. Browne. Rather than placentation and seed coat structure, which are common characteristics used to identify clades in other *Rubiaceae* lineages, fruit morphology, karyology, and pollen morphology appeared to be more useful characters for distinguishing these three main clades. The *Cruckshanksia* clade, the smallest of the three, shares chartaceous, loculicidal capsules, or papery, dehiscent fruits, a strictly pentamerous perianth, and spheroidal, three-colporate pollen grains with simple reticulate tecta. Additionally, most members have yellow flowers. The *Coccocypselum* clade is characterized by colporate pollen grains with complex reticulate tecta. Further, all genera in the clade, except *Coccocypselum*, are characterized by septicidal fruit dehiscence, which is an uncommon trait in *Rubioideae* (Löfstrand et al., 2019).

The final clade, which is the largest and most relevant to this study, is the *Coussarea-Faramea* clade. It includes approximately 270 species, making it the predominant clade in the *Coussareeae* tribe (Löfstrand et al., 2019). Members are widespread in the neotropics, mostly growing in forest biomes, with a broad ecological amplitude ranging from arid or seasonally dry forests to humid and swampy

rainforests. Because of their large numbers, both genera show great species diversity (Löfstrand et al., 2019). The two genera that make up this clade have a sister relationship, as they both share a common ancestor, and they are primarily characterized by porate pollen grains with annuli bordering the pores, two characters uncommon for *Rubiaceae* (Löfstrand et al., 2019). They are also characterized by single-seeded drupaceous fruits with thin endocarps and tetramerous floral corollas (Löfstrand et al., 2019). These two genera differ primarily in the following features: *Coussarea* species contain stipules that are smooth and not aristate, have fruits that are spongy or thickly fleshy and white to yellow, and have pyrenes that lack pre-formed germination slits, while in *Faramea*, costate and aristate stipules are common, fruits are blue to black and leathery or thinly juicy, and seeds have pre-formed germination slits (Taylor and Jardim, 2020).

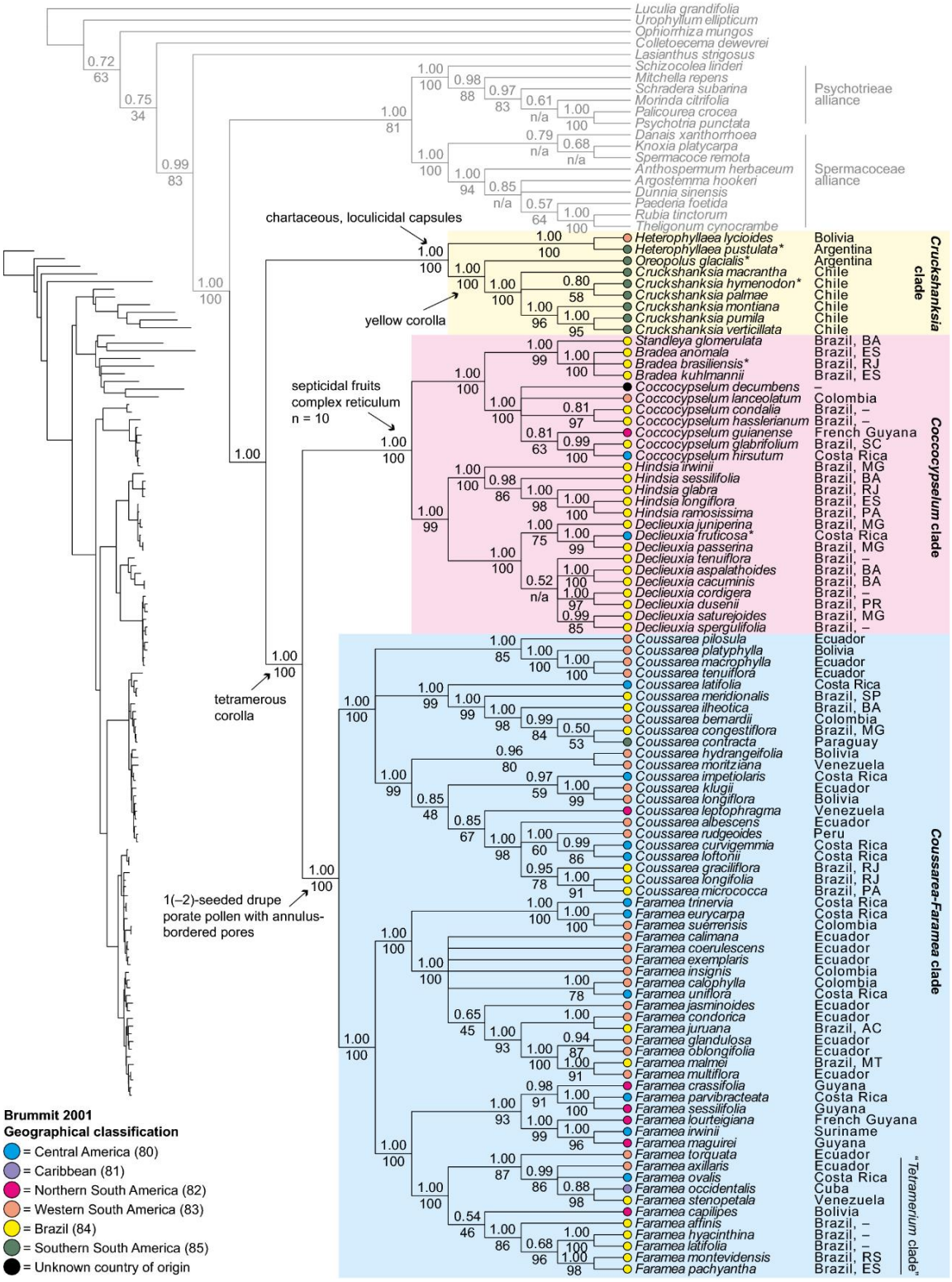

Figure 3: Results of concatenated cDNA + rDNA analyses; Bayesian 50% majority rule consensus cladogram for the tribe *Coussareeae*. Node support is presented to the left of each node (Bayesian posterior probabilities above; maximum likelihood bootstrap values below). Colored circles represent specimen's biogeographic origin. Modified from Löfstrand et al., 2019.

1.1.4 Genus: *Faramea*

The genus *Faramea* consists of 170 species of woody plants of varying growth habit, ranging from shrubs to medium sized trees (Govaerts, 2017). The genus is distributed from central Mexico and the Antilles to Paraguay, where its species inhabit areas from sea level to the high-altitude tree line and can grow in both humid and arid vegetation patches (Govaerts, 2017). *Faramea* shows particularly high diversity throughout the Atlantic Forest region of Brazil and has centers of diversity throughout South America (Löfstrand et al., 2021). As is true of many *Rubioideae* members, *Faramea* is characterized by raphides in its tissues. Additional characteristics of the genus include white or blue, tetramerous corollas and blue-black, fleshy fruits with a single, large pyrene fruitstone, as well as opposite leaves and interpetiolar awned stipules (Löfstrand et al., 2021). As is typical for the *Coussareeae* tribe, the inflorescences can be highly variable, from single to cymose and showy to inconspicuous (Löfstrand et al., 2019).

Figure 4 illustrates the genus *Faramea* divided into two major clades: A and B. Clade A mostly consists of species from southern Central America and western South America, while Clade B includes species from the entire geographic range of *Faramea*. The majority of the species in subclade B1 range from the Guianas through the southern Amazon basin, while those of B2 are primarily found in South America (Löfstrand et al., 2021). Like *Coussareeae*, *Faramea* is characterized by its morphological heterogeneity. The morphological features historically used to classify infrageneric sections in *Faramea*, including stipule form, inflorescence structure, the absence vs. presence of well-developed inflorescence bracts and the shape of the calyx limb, seem not to be of diagnostic value to any of the major clades recovered in the phylogenetic tree. In other words, the morphological characteristics of *Faramea* species are simply too varied and are not indicative of the evolutionary history of the clades as a whole. The study asserts that varied morphological diversity facilitates ecological adaptation and may be correlated with the wide species diversification in *Faramea*, so perhaps these species show interesting ecological roles that have not yet been studied (Löfstrand et al., 2021). Nevertheless, the phylogenetic tree is strongly supported by molecular data and provides insight into the relationships between species. Of particular importance to this study, the species of interest, *F.*

tamberlikiana, is part of Clade B, subclade B1. The species shows a recent common ancestor with *F. sessifolia* P.H. Allen and is more distantly related to *F. boomii* Steyerm.

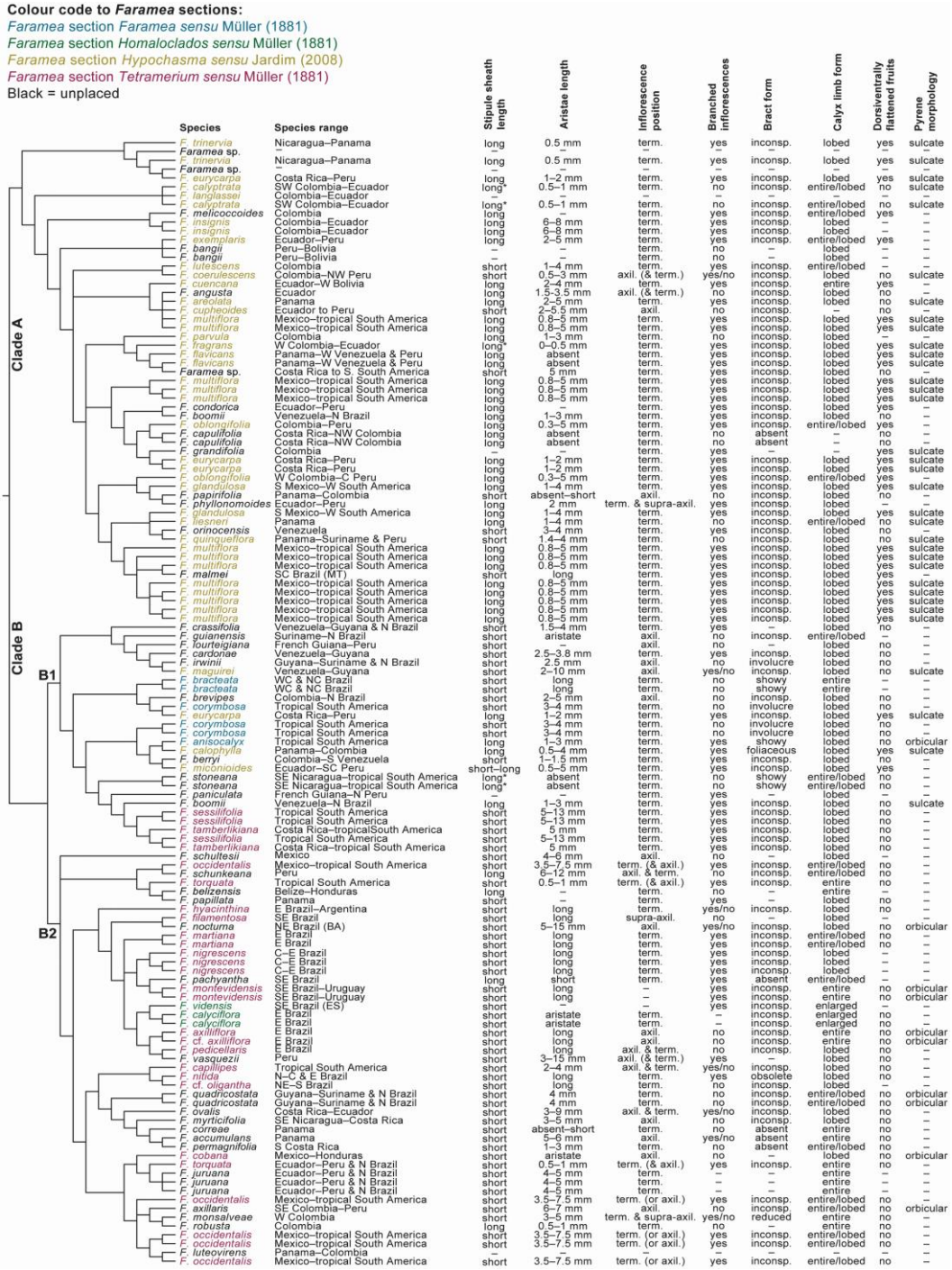

Figure 4: Species level distribution and morphology scored against the phylogenetic tree. Morphological characters utilized to delimit infrageneric sections in *Faramea* scored against a pruned cladogram. 128 samples of *Faramea* encompassing 80 species were used. Modified from Löfstrand et al., 2021.

1.1.5 *Faramea tamberlikiana*

Faramea tamberlikiana—is the primary species of interest for this study. It is a woody perennial tree or small shrub that is distributed throughout central and south America (Govaerts, 2017). It grows no farther north than Costa Rica and can be found all over tropical regions as far south as Bolivia (Govaerts, 2017). *Faramea tamberlikiana* inhabits humid forest understories in both mature and new growth forests at low elevations (Osa Conservation Campus, 2022). The species displays four-petaled, blue to purple flowers organized in showy inflorescences (Figure 5A and 5C) that bloom from February to July (Osa Conservation Campus, 2022). Each flower later develops into a black berry (Figure 5B) which is both edible to humans and widely consumed by bird species (Osa Conservation Campus, 2022). Easily recognizable are the simple pinnate leaves organized in opposite pairs (Figure 5A).

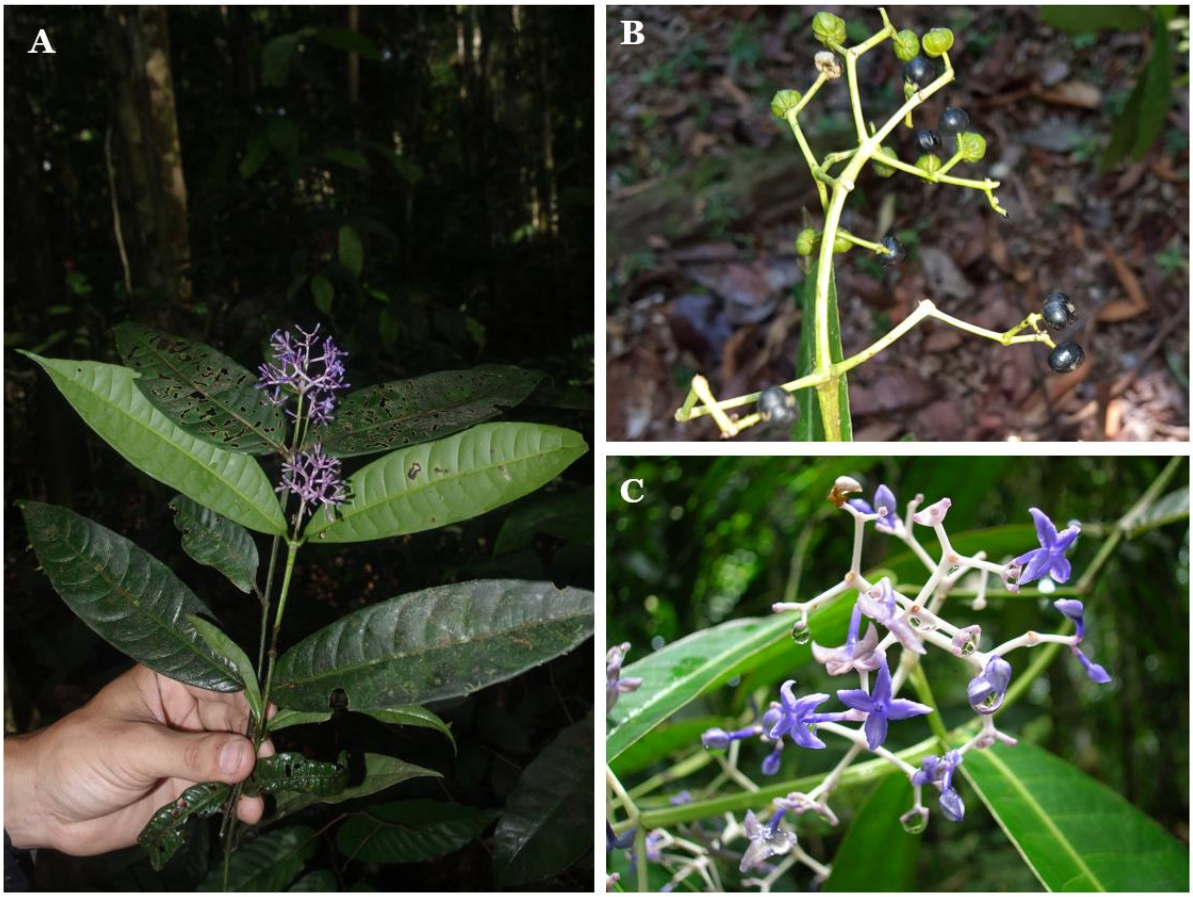

Figure 5: A: photograph of *Faramea tamberlikiana* showing its leaves and inflorescence, adapted from Dávila 2024. B: photograph of the berries from *F. tamberlikiana*, adapted from Osa Conservation Campus 2022. C: closeup photograph of the inflorescence of *F. tamberlikiana*, adapted from Osa Conservation Campus 2022.

1.2 Specialized Metabolism

1.2.1 General

Specialized plant metabolism (SPM) refers to the intricate and, often, highly specific ways that plants have evolved to produce a diverse array of (secondary) metabolites. Secondary metabolites are distinct from primary metabolites in that primary metabolites are necessary for basic plant growth and reproduction, and include functions like photosynthesis, carbon assimilation, respiration, and amino acid biosynthesis; these metabolites are highly conserved and ubiquitous throughout the plant kingdom (Pott et al., 2019). On the other hand, specialized metabolites serve specific functions in ecological interactions, defence mechanisms, and adaptations to various environmental stresses, and can be specific to a certain family, genus, or particular species of plant (Tissier et al., 2014). For this reason, the term "secondary metabolites" is a misnomer: these compounds are essential for plant survival. They play a vital role in facilitating key aspects of primary metabolism (PM), such as attracting pollinators and aiding in seed dispersal, processes without which plant survival would be impossible (Pott et al., 2019). Further, the biosynthesis of these compounds often occurs in specific plant tissues and can be upregulated to suit particular conditions, which demonstrates the complexity and adaptability of these compounds to combat environmental stresses (Tissier et al., 2014).

The SPM is always derived from the primary, which means that the PM provides the fundamental building blocks and precursors necessary for the synthesis of specialized metabolites, as shown in Figure 6 (Pott et al., 2019). Compounds such as sugars, amino acids, and organic acids, as well as intermediates of central metabolic pathways, including glycolysis, the citric acid cycle, and the shikimate pathway, serve as starting materials or substrates from which specialized metabolites can be produced (Pott et al., 2019). These various precursor molecules undergo enzymatic transformations, often involving specialized biosynthetic routes, to produce a diverse array of specialized metabolites (Vogt, 2010). The enzymes involved in these pathways, including terpene synthases, polyketide synthases, and alkaloid biosynthetic enzymes, catalyse specific reactions that modify and rearrange the primary metabolites into specialized metabolites containing distinct chemical structures and properties (Pott et

al., 2019; Vogt, 2010). While the PM is essential for the basic functioning and growth of plants, the SPM diversifies their biochemical repertoire and allows them to survive in their environment.

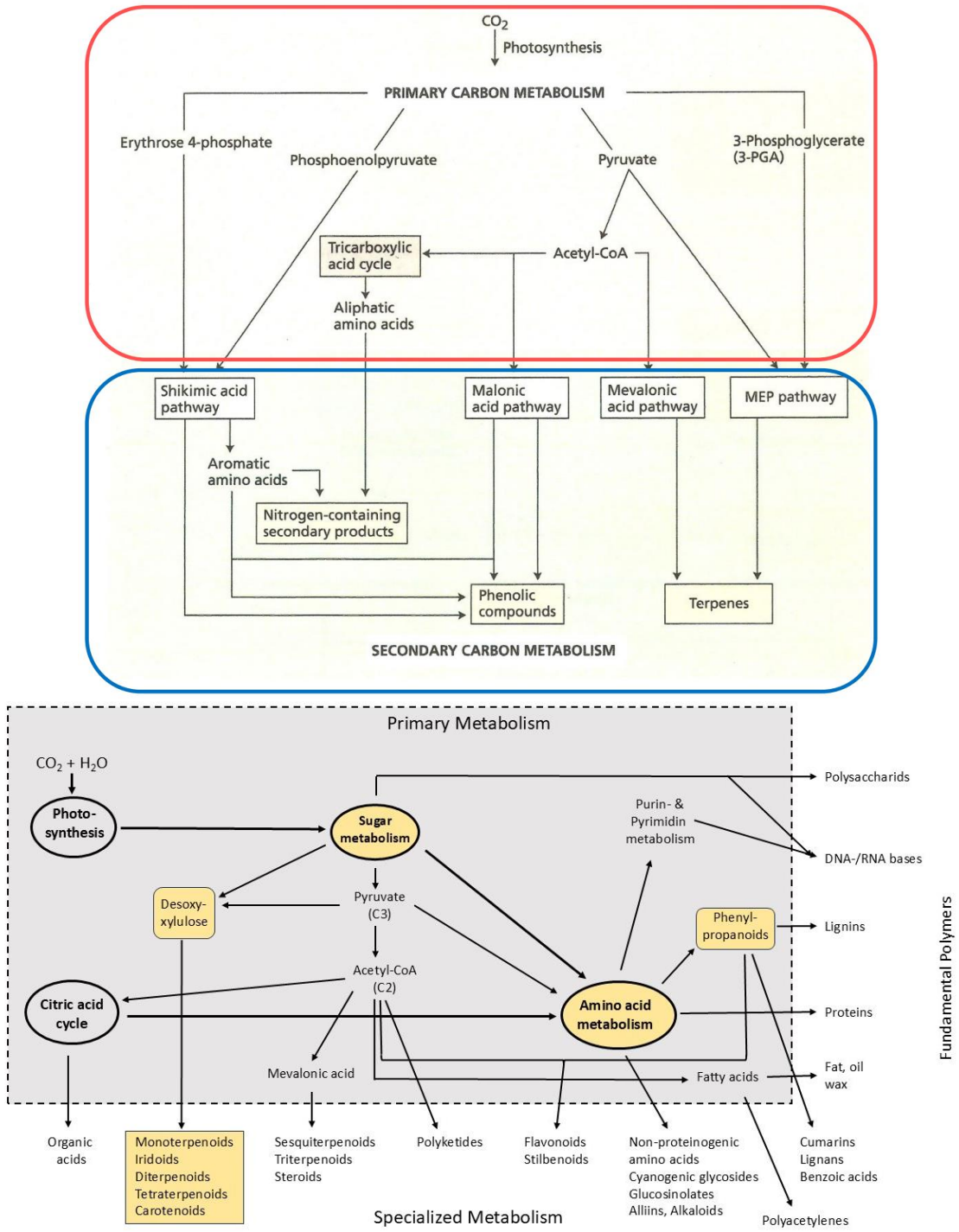

Figure 6: General pathways for the transformation of primary metabolic building blocks into specialized metabolites, modified from Taiz and Ziegler, 2010. The top figure depicts simplified pathways while the bottom figure includes more specific pathways and highlights those of importance to the study.

1.2.2 Terpenoids

The most prominent classes of specialized metabolites include alkaloids, terpenoids, and phenolic compounds and can be broadly categorized by their origins in the PM (Tissier et al., 2014). Many specialized metabolites, such as terpenoids, originate from sugar metabolism, representing the first major branching point in specialized metabolism. The next significant branch arises from the shikimate pathway, which gives rise to alkaloids, pseudoalkaloids, and glucosinolates. Some metabolites, like phenolic compounds such as flavonoids, are synthesized through a combination of both pathways (Vogt, 2010).

Terpenoids represent one of the largest and most significant classes of specialized metabolites, with over 25,000 identified to date (Tissier et al., 2014). The fundamental building blocks of terpenoids are isoprene units, which are five-carbon branched chains (Tissier et al., 2014). Terpenoids are classified based on the number of C5, or isoprene, units they contain (Tissier et al., 2014). The great structural diversity of terpenoid compounds arises from the variability in the arrangement, modification of these isoprene units, and the number of C5 units involved. The broad substrate specificity of terpene synthases and cyclases further enhances this diversity, allowing for interactions with other biosynthetic pathways. Terpenoid synthesis often intersects with alkaloid biosynthesis, particularly in the production of compounds such as iridoids and indole alkaloids (Cherney and Baran, 2011).

Terpenoids are derived from either the mevalonic acid (MVA) or the methyl-D-erythritol phosphate (MEP) pathway, both of which come from the sugars of the PM (Tissier et al., 2014). The MEP pathway is responsible for monoterpene, diterpene, and tetraterpene biosynthesis, while the MVA pathway leads to sesquiterpenes, triterpenes, and sterols (Tissier et al., 2014). The MVA pathway takes place in the cytosol and derives from acetyl-coenzyme A, or CoA (Tzin and Galili, 2010). Acetyl-CoA has the primary metabolic function of delivering an acetyl group (C2-body) to the citric acid, or Krebs, cycle, enabling cellular respiration and energy generation. In the SPM, acetyl-CoA serves as a building block for the biosynthesis of a wide range of specialized metabolites, which originate from the condensation and subsequent modification of acetyl-CoA molecules. Acetyl-CoA typically comes from the breakdown of carbohydrates via glycolysis, where pyruvate loses a carboxyl group as carbon

dioxide and the remaining molecule is oxidized, leaving behind an acetyl group and Coenzyme A. These molecules combine to form acetyl-CoA, which, if it is not used in the Krebs cycle to generate energy, can serve as a precursor for the biosynthesis of a variety of specialized metabolites. In the MVA pathway, two molecules of acetyl-CoA condense in the presence of acetyl-CoA acetyltransferase (AACT) to form acetoacetyl-CoA, which is then converted to hydroxymethylglutaryl-CoA in a reaction catalyzed by hydroxymethylglutaryl-CoA synthase (HMGS), and ultimately reduced to mevalonate via HMG-CoA reductase, or HMGR (Tissier et al., 2014; Liao et al., 2016). Mevalonate then undergoes several phosphorylation steps, catalyzed by either mevalonate kinase (MK) or phosphomevalonate kinase (PMK), to form mevalonate-5-diphosphate. This molecule undergoes a final conversion, in the presence of diphospho-mevalonate decarboxylase (PPMD), to form isopentenyl diphosphate (IPP) and, in smaller quantities, its isomer dimethylallyl diphosphate, or DMAPP (Tissier et al., 2014; Liao et al., 2016).

On the other hand, the MEP pathway takes place in the chloroplasts and begins with glyceraldehyde-3-phosphate (G3P) and pyruvate, both of which are derived from the Calvin cycle (Tissier et al., 2014). These two molecules condense in the presence of 1-deoxy-D-xylulose-5-phosphate (DXS) to form 1-deoxy-D-xylulose5-phosphate (DXP), which, when catalyzed by 1-deoxy-D-xylulose 5-phosphate reductoisomerase (DXR), is reduced to 2C-methyl-D-erythritol-4-phosphate, or MEP (Tissier et al., 2014; Liao et al., 2016). A cytidyl nucleotide is then added, in the presence of 2C-methyl-D-erythritol-4-phosphate cytidyl transferase (MCT), to form 4-(cytidine-5′-diphospho)-2Cmethyl-D-erythritol (CDP-ME), which is phosphorylated to 4-diphosphocytidyl-2C-methyl-D-erythritol-4-phosphate (CDP-MEP), aided by 4-diphosphocytidyl-2C-methyl-D-erythritol kinase, or CMK (Tissier et al., 2014). The formed CDP-MEP undergoes further cyclization to 2C-methyl-D-erythritol-2,4-cyclodiphosphate (ME-cPP) via 2C-methyl-D-erythritol-2,4-cyclodiphosphate synthase (MDS) and is then reduced to 4-hydroxy-3-methylbut-2-enyl diphosphate (HMBPP) in the presence of 1-hydroxy-2-methyl-2-(*E*)-butenyl-4-diphosphate synthase, or (HDS) (Tissier et al., 2014). Finally, HMBPP is reduced to IPP or DMAPP in a reaction catalysed by 1-hydroxy-2-methyl-2-(*E*)-butenyl-4-diphosphate reductase, or HDR (Tissier et al., 2014). The MEP pathway plays a crucial role as it leads to the formation of geranyl

diphosphate (GPP), an important intermediate and terpene backbone (Tissier et al., 2014).

1.2.2.1 Iridoids

Iridoids are a specific subgroup of monoterpenes characterized by a cyclopentanopyran ring (Seigler, 1998). Iridoids are found predominantly in plants, especially those of the *Lamiaceae*, *Loganiaceae*, and *Rubiaceae* families, and most commonly function in plant-insect interactions (Seigler, 1998). These compounds contribute to the ecology of landscapes by serving as a defense mechanism against herbivores and pathogens, largely due to their bitter taste and potential toxicity. Seco-iridoids, like secologanin, are a class of iridoid compounds characterized by the cleavage of the cyclopentane ring, which results in an open ring structure (O'Connor and Maresh, 2006). Secologanin is additionally important because it serves as one of the key precursors in the mixed biosynthesis pathway that leads to monoterpene-indole alkaloids (O'Connor and Maresh, 2006).

The first step in iridoid synthesis (Figure 7) is the condensation of isopentyl diphosphate (IPP) and dimethylallyl diphosphate (DMAPP), catalyzed by *trans*-isoprenyl diphosphate synthase (IDS), to form geranyl diphosphate (Miettinen et al., 2014). Geranyl diphosphate (GPP) is the fundamental precursor involved in the biosynthesis of all terpenoids and its formation occurs via the MEP, or deoxyxylulose, pathway.

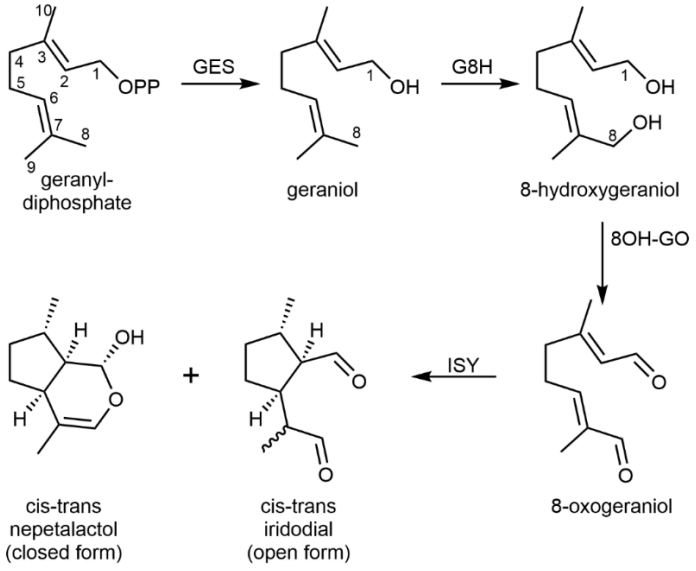

Figure 7: Biosynthesis of iridodial the key precursor of iridoids. Modified from Sherden et al. 2017.

Next, GPP is hydrolyzed to geraniol by the enzyme geraniol synthase (GES) (Miettinen et al., 2014). Both steps take place in specialized plastids, often in plant trichomes. Geraniol goes through a hydroxylation reaction catalyzed by geraniol-8-hydroxylase (G8H) to form 8-hydroxygeraniol, which is then oxidized by 8-hydroxygeraniol oxidase (HGO) to 8-oxogeranial (Miettinen et al., 2014). There is then a two-step reduction and cyclization reaction that ultimately results in nepetalactol and iridodial isomers (Miettinen et al., 2014).

1.2.2.2 Apocarotenoids

Apocarotenoids, or megastigmanes, are terpenoid compounds formed through the oxidative cleavage of carotenoids (Wang et al., 2018; Hou et al., 2016). Carotenoids are large compounds usually related to pigmentation and often function as photoprotective or attractive to pollinators (Hou et al., 2016). Apocarotenoids are smaller molecules, which are often more soluble and volatile, and typically serve a signaling function (Hou et al., 2016).

Apocarotenoids are an end product of carotenoid formation, which occurs via the MEP pathway, beginning with the condensation of IPP and DMAPP to form geranylgeranyl pyrophosphate, or GGPP (Miettinen et al., 2014). Two molecules of GGPP are condensed in the presence of phytoene synthase (PSY) to form phytoene (Hou et al., 2016). This molecule undergoes desaturation catalyzed by phytoene desaturase (PDS) and zeta-carotene (ζ-carotene) isomerase (ZISO) to form ζ-carotene (Hou et al., 2016). Zeta-carotene desaturase (ZDS) catalyzes the reaction to neurosporene, and carotenoid isomerase (CRTISO) finalizes the transformation to lycopene (Hou et al., 2016). This serves as a major branching point in carotenoid synthesis: the formation of either α-or β-carotene (Hou et al., 2016). Apocarotenoids can form in many ways, including the oxidative cleavage of phytoene neurosporene, lycopene, and β-carotene products (Hou et al., 2016). The megastigmane of interest in this study, blumenol, follows the pathway of all C_{27} apocarotenoids through α-carotene formation, where lycopene β-cyclase (LCY-β) and lycopene ε-cyclase (LCY-ε) facilitate the formation of α-carotene (Hou et al., 2016). Carotenoid cleavage dioxygenase seven (CCD7) acts on an unknown carotenoid substrate to yield a C_{27} apocarotenoid, which is cleaved further by CCD1 to yield blumenol (Hou et al., 2016).

1.2.3 Alkaloids

Alkaloids are a particularly prominent class of nitrogen-containing compounds, both because of their sheer number and their medical significance, encompassing compounds like morphine and widely used drugs such as nicotine (Tissier et al., 2014). These compounds are primarily synthesized through modifications of amino acids, typically via decarboxylation or deamination processes, and the nature of the specific amino acid involved often determines the class of alkaloid produced (Tissier et al., 2014). The great diversity of alkaloid compounds is a result of both the different combinations of structural transformations on the alkaloid backbones, including methylations, hydroxylations, and oxidations, as well as the varied condensation partners (Tissier et al., 2014).

Alkaloids are classified into various groups based on their biosynthetic origins, many of which derive from aromatic amino acids such as phenylalanine, tyrosine, and tryptophan (Tissier et al., 2014). Tryptophan, for example, serves as a precursor for the large class of indole alkaloids (Tissier et al., 2014). One important subclass is the monoterpene-indole alkaloids, which arise through a mixed biosynthesis pathway, involving the condensation of secologanin, a monoterpene glucoside, and tryptamine, an indole structure derived from tryptophan decarboxylation, usually catalyzed by strictosidine synthase (Berger et al., 2015). This mixed biosynthetic route results in a vast array of chemically diverse compounds, many of which exhibit pharmacological activity (Berger et al., 2022). The broad structural diversity and complex biosynthetic origins of alkaloids make them essential for plant defense.

1.2.4 Phenolics and Polyphenolics

Phenolics are a diverse class of specialized metabolites mostly derived from the shikimate pathway, though some phenolic structures can also originate from alternative pathways, such as the acetate or isoprenoid pathways. They are ubiquitous in the plant kingdom, with their origins tracing back to the time when algae emerged from the sea to colonize land. Phenolics are characterized by an aromatic ring system attached to at least one hydroxyl group, and polyphenolics include several rings and hydroxyl groups; this structure allows for many arrangements and a great diversity of functions. These compounds are crucial for plants to cope with abiotic stresses and

include UV protective compounds, as well as structural elements like lignin. Additionally, compounds like flavanols and anthocyanins are integral to plant pigmentation, and influence the colors of flowers and fruits, which in turn affects pollination and seed dispersal. The extensive range and vital roles of phenolics make them import in both plant physiology and the ecology of an ecosystem (Vogt, 2010).

Simple phenols include benzoic acid derivatives, salicinoids, and coumarins, compounds which most often contribute to biotic plant defense. Polyphenolics include a multitude of subclasses, each with their own structural and functional distinctions. Flavonoids are by far the largest class of polyphenolic compounds. Its major subclasses, including flavanols, flavones, and anthocyanins, play many roles, including flower pigmentation, herbivory defense, antioxidative pathogen protection, and UV protection. Due to their basic structure, these compounds have a high antioxidative potential and can interact with proteins and enzymes. Anthocyanins are red to blue pigments that provide color to flowers, fruits, and young leaves, and may aid in UV protection. Flavonoid-related and other polyphenolic tannins act as bitter feeding deterrents against herbivores. The fundamental polymeric lignin contributes to plant structure and rigidity (Vogt, 2010).

Regardless of subclass, all phenolics covered in this work start in the shikimate pathway (Vogt, 2010). This pathway begins with the conversion of phosphoenolpyruvate (PEP) and erythrose-4-phosphate (E4P) through several enzyme-catalyzed reactions into shikimate and later chlorismate (Tzin and Galili, 2010). Chlorismate is the branching point for the production of the three proteinogenic aromatic amino acids: phenylalanine, tyrosine and tryptophan, as well as other primary and specialized metabolites (Schmid and Amrhein, 1995). In a reaction catalyzed by chlorismate mutase (CM), chlorismate is converted to prephenate, which is then catalyzed by prephenate aminotransferase (PAT) to form arogenate (Tzin and Galili, 2010). Arogenate can then undergo further steps to form either tyrosine or phenylalanine (Tzin and Galili, 2010). From this point, there are two major biosynthetic routes for the production of phenolics: the phenylpropanoid pathway and the flavonoid pathway.

The starting point for the phenylpropanoid pathway is phenylalanine, which forms when arogenate is catalyzed by arogenate dehydratase (Tzin and Galili, 2010).

Phenylalanine then undergoes nonoxidative deamination to synthesize *trans*-cinnamate in the presence of both phenylalanine ammonia lyase and tyrosine ammonia lyase, PAL and TAL respectively (Vogt, 2010). Cinnamate-4-hydroxylase (C4H) catalyses this molecule to form 4-coumarate (= *para*-coumarate), which can be further catalyzed by 4-coumaroyl CoA-Ligase, 4CL (Vogt, 2010). The final step in this pathway, and the point of further branching to other metabolite-formation, is the extremely important molecule, *para*-coumaroyl CoA (Vogt, 2010). As illustrated by Figure 8, *p*-coumaroyl CoA may be used in highly specialized biosynthetic routes to form a diverse array of phenolics including coumarins, lignin and lignans, catechin, stilbenes, phenylpropanoid esters, and phenylpropenes (Vogt, 2010).

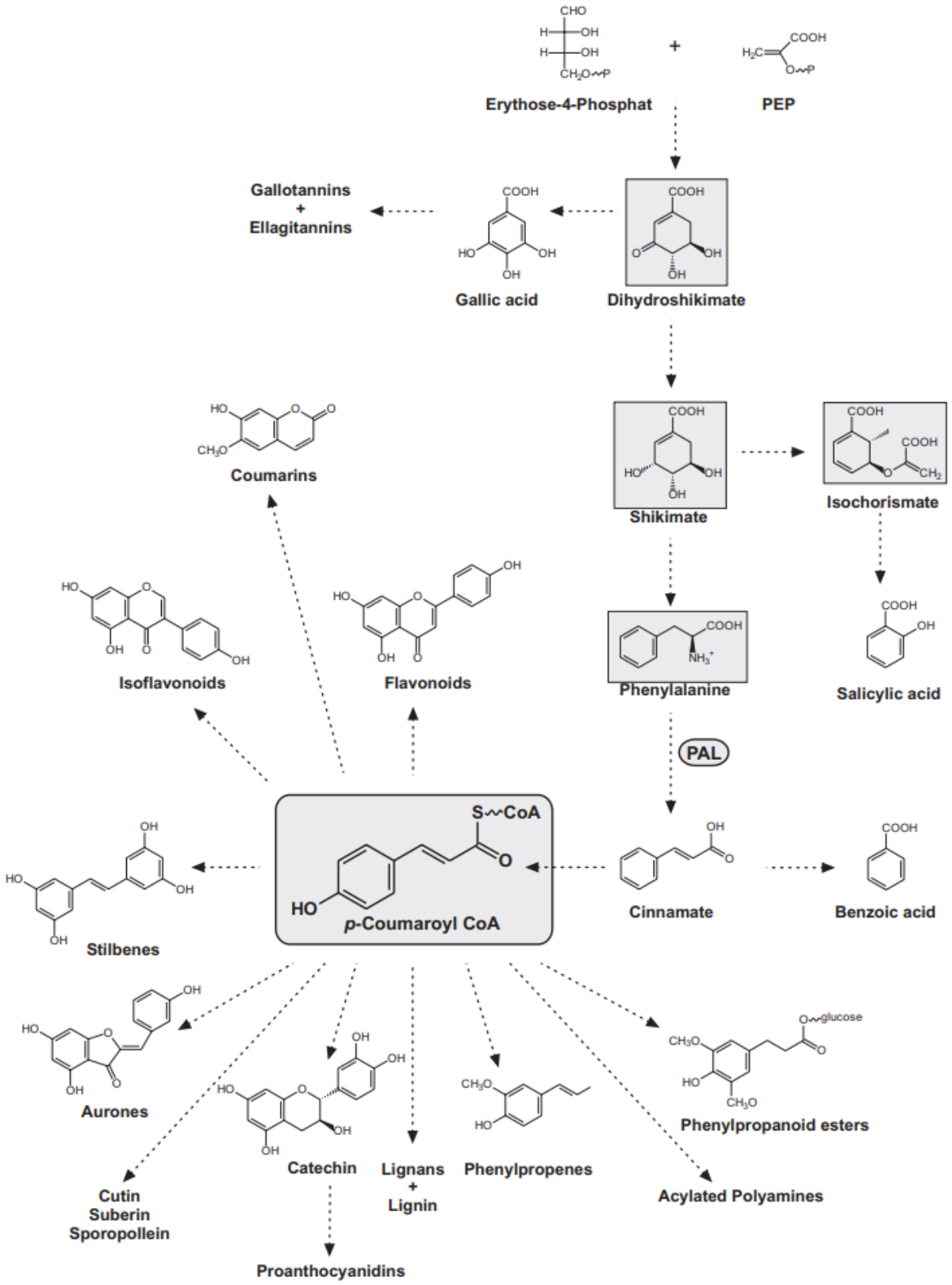

Figure 8: Diversification of phenylpropanoids based on the general phenylpropanoid pathway and transformations of *p*-coumaroyl CoA. Modified from Vogt 2010.

1.2.4.1 Flavonoids and Isoflavonoids

The flavonoid biosynthetic pathway is unique in that it combines both the phenylpropanoid and malonic acid pathways. One molecule of *p*-coumaroyl CoA from the phenylpropanoid pathway combines with three molecules of malonyl-CoA to generate naringenin chalcone in a reaction catalyzed by chalcone synthase, CHS (Liu et al., 2021). Malonyl-CoA, an important intermediate in fatty acid formation, is derived from the acetyl-CoA synthesized in the citric acid cycle (Liu et al., 2021). Chalcone formation acts as the foundational structure for the biosynthesis of subsequent flavonoid compounds (Liu et al., 2021). Chalcones are easily cyclized in the presence of chalcone isomerase (CHI) to form flavanones, including the important compound naringenin (Liu et al., 2021). This process forms the key heterocyclic C ring characteristic of the flavonoid pathway (Liu et al., 2021).

Flavones can be synthesized from flavanones by flavone synthase (FNS), which catalyzes double-bond formation between positions C2 and C3 on the C ring (Liu et al., 2021). Isoflavones, a compound class mostly restricted to legumes, are produced via several enzymatic transformations that ultimately result in a double bond between C2 and C3, as well as a shift of the B ring from position C2 to position C3 on the C ring (Liu et al., 2021). Dihydroflavonols, or flavanonols, are an important flavonoid that are converted from flavanone through catalysis of flavanone 3-hydroxylase (F3H) and may undergo further transformation to flavanols (Liu et al., 2021). Flavonols are metabolites with a hydroxylated C3 position; they can be synthesized from flavanonols by flavonol synthase, FLS (Liu et al., 2021). Flavonols are of widespread occurrence, and they are mostly accumulated as glycosides.

As with all flavonoid compounds, the isoflavone pathway begins with one molecule of *p*-coumaroyl CoA from the phenylpropanoid pathway and three molecules of malonyl-CoA to form naringenin chalcone, the core structure of flavonoid compounds (Liu et al., 2021). The enzyme chalcone isomerase (CHI) catalyzes cyclization to form flavanones, including naringenin, liquiritigenin, and eriodictyol, which act as the branching point and shared substrate for flavone, isoflavone, and phlobaphene pathways (Liu et al., 2021). Isoflavone synthase (IFS) catalyzes the transformation from flavanones and can use both naringenin and liquiritigenin as substrates to generate 2-hydroxy-2,3-dihydrogenistein and 2,7,4′-trihydroxyisoflavanone,

respectively (Liu et al., 2021). These compounds can be converted into isoflavone genistein and daidzein in the presence of hydroxyisoflavanone dehydratase (HID) (Liu et al., 2021). The result of the catalyzing enzymes IFS and HID is a double bond formation on the C-ring between positions C2 and C3, as well as a shift of the B-ring from C2 to C3 (Liu et al., 2021).

1.2.4.2 Coniferyl Alcohol and Eugenol

The first step in the biosynthesis of coniferyl alcohol begins with the crucial phenolic intermediate, *p*-coumaroyl CoA (Metsämuuronen and Sirén, 2019). In the presence of C3H (*p*-coumarate 3-hydroxylase), this compound is hydroxylized to caffeoyl CoA, which then undergoes methylation via caffeoyl-CoA O-methyltransferase (CCoAOMT) to feruloyl-CoA (Metsämuuronen and Sirén, 2019). Cinnamoyl CoA reductase (CCR) catalyzes the reduction of feruloyl CoA to coniferyl aldehyde, which is further reduced by cinnamyl alcohol dehydrogenase (CAD) to form coniferyl alcohol (Metsämuuronen and Sirén, 2019). From this point, coniferyl alcohol can undergo further transformation steps to synthesize lignans, which are essential for deterring herbivory, and serve as precursors for cinnamic acid derivatives like eugenol. (Metsämuuronen and Sirén, 2019)

Eugenol biosynthesis starts with coniferyl alcohol as the primary substrate, which is catalyzed in the presence of coniferyl alcohol acyltransferase, or CFAT (Koeduka et al., 2006). A nucleophilic displacement mechanism takes place, where a hydrogen ion from NADPH facilitates the reduction process (Koeduka et al., 2006). This occurs alongside the removal of an acyl leaving group (Koeduka et al., 2006). The negatively charged transition state of the acyl group may be stabilized by proton donation, leading to the transformation of coniferyl alcohol into coniferyl acetate (Koeduka et al., 2006). Afterwards, coniferyl acetate is catalyzed by eugenol synthase to form eugenol (Koeduka et al., 2006). This compound would then undergo further transformations, such as hydroxylation or methylation and glycosylation to form the species found.

The isolated compounds **1** and **2** are closely related to eugenol, as they share a common biosynthetic pathway originating from the transformation of phenylalanine to cinnamatic acid and subsequently to *p*-coumaroyl CoA (Vogt, 2010). Further, hydroxychavicol (**1**) and 2-methoxy-4-(2-propen-1-yl)phenyl-6-*O*-D-apio-β-D-

furanosyl-β-D-glucopyranoside (**2**) likely follow the eugenol biosynthetic pathway, which progresses through the intermediate coniferyl alcohol (Metsämuuronen and Sirén, 2019). These three molecules are structurally similar, as they all share the typical cinnamic acid-derived phenylpropanoid backbone, and differ mainly in the position and type of functional groups attached. While eugenol has a methoxy group at the position C-2, hydroxychavicol (**1**) has a hydroxyl group at the same position. On the other hand, 2-methoxy-4-(2-propen-1-yl)phenyl-6-*O*-D-apio-β-D-furanosyl-β-D-glucopyranoside (**2**) is a glycosylated phenylpropanoid derivative with an attached glucose molecule, which enhances its solubility and more easily allows for storage within plant tissues without altering the core molecular structure.

1.2.5 Phytochemistry of *Rubiaceae*

One important aspect of the *Rubiaceae* family, and of particular interest for this study, is its notable and extensive chemodiversity. Many *Rubiaceae* plants produce varied specialized metabolites, including alkaloids, iridoids, anthraquinones, triterpenes, and indole alkaloids (Martins and Nunez, 2015). This diverse chemical profile plays a crucial role in the family's ecological interactions, medicinal applications, and economic significance. The role of diversified chemicals is so ubiquitous in *Rubiaceae* that chemotaxonomic markers have been used to aid in the identification and classification of plants into genera and subfamilies (Martins and Nunez, 2015). Alkaloids, one prominent class of compounds in the family, exhibit various physiological effects and often serve as a defence mechanism against herbivores. Alkaloids are responsible for some of the best-known compounds in *Rubiaceae*, including caffeine from coffee (*Coffea* spp.), and the anti-malarial drug quinine from *Cinchona* species (Martins and Nunez, 2015).

Within *Rubiaceae*, some phytochemicals may serve as valuable taxonomic markers, which help differentiate various genera and species (Martins and Nunez, 2015). The presence of specific specialized metabolites, such as alkaloids, iridoids, and anthraquinones, can be indicative of particular taxonomic groups and shed light on their evolutionary relationships (Martins and Nunez, 2015). Additionally, some studies have shown that primary metabolites such as leaf fatty acids are also good indicators phylogenetic distinctions in *Rubiaceae* (Mongrand et al., 2005). Given the

fraught classification history of this family, utilizing phytochemicals as taxonomic markers may enhance the accuracy of classification by revealing chemical signatures unique to specific lineages. This approach may be particularly important in tribes like the *Coussareeae*, where traditional morphology alone is insufficient to sort out the evolutionary relationships in structurally divergent lineages.

In a 2015 review of prior phytochemical studies on *Rubiaceae*, data was compiled to identify chemotaxonomic trends within the family (Martins and Nunez, 2015). These data support the three-subfamily classification, which includes *Ixoroideae*, *Cinchonoideae*, and *Rubioideae*. The *Ixoroideae* subfamily is predominantly characterized by the presence of iridoids, while the *Cinchonoideae* subfamily produces indole alkaloids most prominently (Martins and Nunez, 2015). In *Rubioideae*, anthraquinones dominate the chemical profile, but, because it is the largest and most ancient of all lineages, also shows a greater compound diversity than the other two subfamilies (Martins and Nunez, 2015). A separate phytochemical review suggested that the compounds 10-deacetylasperulosidic acid and asperuloside, both iridoids, are characteristic in nearly all *Rubioideae* subfamily species (Wolff et al., 2019). A uniting factor in all three subfamilies is abundant production of widespread occurring triterpenes, as such these compounds cannot serve as chemotaxonomic markers (Martins and Nunez, 2015).

Among the *Rubioideae* members, the *Psychotrieae* alliance stands out as a major producer of alkaloids, with all prior phytochemical studies on genera within this tribe resulting in the isolation of these compounds (Martins and Nunez, 2015). A notable feature of *Psychotrieae* is that many species produce compounds that impact the central nervous system (Martins and Nunez, 2015).

More recent phytochemical reviews have provided insight into the relationship between compound accumulation and taxonomy: Berger et al. (2022) provided classification of the *Palicourea* alkaloids, which predominantly consisted of monoterpene-indole alkaloids, and outlined potential biosynthetic relationships based on biosynthetic pathways and molecule-specific structural changes (Berger et al., 2022). Additionally, a study on the phytochemical differentiation between *Psychotrieae* and *Palicoureeae* highlighted several tribe-specific compound accumulation patterns, emphasizing the importance of including chemical data in

taxonomic studies (Berger et al., 2021). Specifically, the *Psychotrieae* tribe was characterized mainly by polyphenols and tannin accumulation, while *Palicourea* primarily synthesized indole alkaloids and monoterpene indole alkaloids (Berger et al., 2021). Although further data is required to confirm phylogenetic distinctions, some patterns linking taxonomy to alkaloid accumulation have been identified (Berger et al., 2022).

1.2.6 Phytochemistry of *Faramea* Species

Data was compiled from all known phytochemical studies of *Faramea* species, and it became apparent that all species studied accumulated phenolic compounds or iridoids, or a mix of both, as shown in Table 1. The main iridoids present were 10-deacetylasperulosidic acid, a compound characteristic of *Rubioideae* family members, and monotropein (Barboza et al., 2018; Wolff et al., 2019). The primary phenolic compounds were flavanones and flavanols in *F. bahiensis*, *F. hyacynthina*, and *F. truncata* (Barboza et al., 2018; Wolff et al., 2018; Wolff et al., 2019). In *F. guianensis*, flavan derivatives dominated, and in *F. cyanea*, anthraquinones were most prevalent (Sauvain et al., 1994; Ferrari et al., 1985). While it cannot be certain that these compounds play a definitive role in the chemical ecology of *Faramea*, it is intriguing that these species lack the alkaloids that are so prominent in other *Rubioideae* members. Additionally, flavonol glycosides, based on the aglycones quercetin and kaempferol, are common in the related *Psychotrieae* alliance, suggesting a possible chemotaxonomic relationship (Berger et al., 2016).

Iridoids

Nepetalactol, derived from the general iridoid pathway, serves as the precursor for the seco-iridoid biosynthetic pathway, which is particularly significant in *Faramea*. Although its intermediary steps are not entirely settled, the likely path is that the *cis-trans*-iridodial and *cis-trans*-nepatalalactol molecules are converted into an iridotrial intermediate (Miettinen et al., 2014). In the presence of iridoid oxidase (IO), this molecule is transformed into 7-deoxyloganetic acid; a glucose molecule is then added and 7-deoxyloganic acid is formed (Miettinen et al., 2014). From this point, the compound is decarboxylated to loganic acid in a reaction catalyzed by 7-deoxyloganic

acid hydroxylase (7-DLH). Through further steps, loganic acid can undergo transformation to secologanin and later important compounds like strictosidine (Miettinen et al., 2014). However, in the case of *Faramea*, loganic acid undergoes hydroxylation to geniposidic acid and further transformations take place to form the relevant iridoid species, as illustrated by Figure 9 (Mitova et al., 2002).

Deacetylasperulosidic acid is an iridoid glycoside synthesized through a pathway starting with the formation of GPP via the MEP pathway, followed by sequential enzymatic steps which ultimately lead to the production of loganic acid. Loganic acid can be transformed into deacetylasperulosidic acid; although the steps of this pathway are not entirely settled, one proposed route takes place through the formation of geniposidic acid as an intermediate, which can be further transformed into deacetylasperulosidic acid and related iridoid species, as shown in Figure 9 (Mitova et al., 2002).

In *Faramea*, 10-deacetylasperulosidic acid is known in *F. bahiensis*, *F. hyacynthina*, and *F. truncata* (Barboza et al., 2018; Wolff et al., 2018; Wolff et al., 2019). Monotropein is found in *F. bahiensis* and *F. hyacynthina*, and the related monotropein methyl ester is additionally found in *F. hyacynthia* (Wolff et al., 2019). Additionally, asperuloside was found in *F. truncata* (Barboza et al., 2018). As illustrated by Figure 9, these are closely related iridoid glycosides which stem from the precursor loganic acid (Mitova et al., 2002).

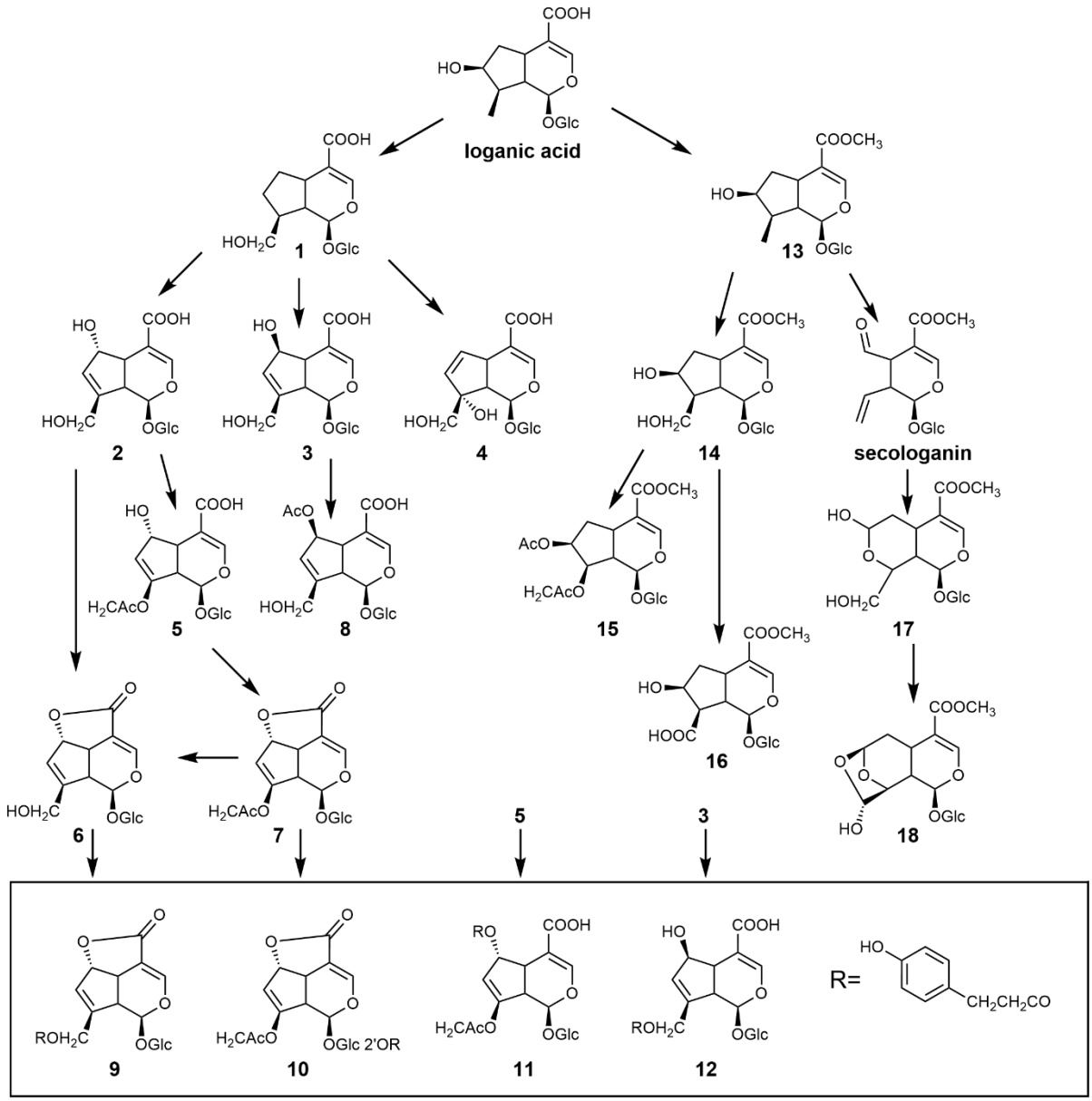

Figure 9: Iridoids and secoiridoids isolated from *Galium* species and their probable biosynthetic linkages. Geniposidic acid (1), 10-deacetylasperulosidic acid (2), scandoside (3), monotropein (4), asperulosidicacid (5), deacetylasperuloside (6), asperuloside (7), 6-*O*-acetylscandoside (8), V1-iridoid (9), V2-iridoid (10), humifusin B (11), humifusin A (12), loganin (13), 10-hydroxyloganin (14), 7-*O*-acetyl-10-acetoxyloganin (15), 7-hydroxy-11-methylforsythide (16), 10-hydroxymoronoside (17), secogalioside (18). Modified from Mitova et al. 2002.

Table 1: All known compounds isolated from *Faramea* species based on a literature survey.

Species	Plant Parts	Compound	Name	Class	Source
		β-sitosterol		Steroid	
		3,4-dihydro-3-hydroxy-2,2-dimethyl-2H-naphtho[1,2-b]pyran	Faramol	Naphthopyran Derivative	
		3,4-dihydro-3-hydroxy-7-methoxy-2,2dimethyl-2H-naptho[1,2-b]pyran	7-methoxyfaramol	Naphthopyran Derivative	
		1,3-Dihydroxy-2-methylanthraquinone	Rubiadin	Anthraquinone	
		3-hydroxy-2-methylanthraquinone		Anthraquinone	
		3-hydroxy-1-methoxy-2-methoxymethylanthraquinone	damnacanthol-ω-methyl ether	Anthraquinone	
F. cyanea	Heartwood (benzene extract)	1,3-dihydroxy-2-methoxymethylanthra-quinone	lucidin-ω-methyl ether	Anthraquinone	(Ferrari et al., 1985)
		5,7,4'-trihydroxyflavan		Flavan	
F. guianensis	Leaves (CH2Cl2 then EtOAc)	5,7-dihydroxy-4'-methoxyflavan		Flavan	(Sauvain et al., 1994)
		4-*O*-methyldihydrodehydrodiconiferyl alcohol (3',4-di-0-methylcedrusin)	dihydrobenzofuran lignan	Lignan	
F. salicifolia (F. multiflora)	Aerial parts (EtOH extract)	3,4,2'-trihydroxy-4'-methoxychalcone	Calythropsin	Chalcone	(Ross et al., 1998)
F. bahiensis	Leaves (MeOH extract)	5-hydroxy-4'-methoxy-flavanone-7-*O*-ß-D-apiofuranosyl-(1→6)-ß-D-glucopyranoside		Flavanone	
		5,4'-dihydroxy-flavanone-7-*O*-ß-D-apio-furanosyl-(1→6)-ß-D-glucopyranoside		Flavanone	
		5,3',5'-trihydroxy-flavanone-7-*O*-ß-D-glucopyranoside		Flavanone	(Nascimento et al., 2017)
		(2S)-isosakuranetin-7-*O*-ß-D-apiofuranosyl-(1→6)-ß-D-glucopyranoside	4'Me naringenin	Flavanone	
		(*E*)-3-(3,4-dihydroxyphenyl)prop-2-enoic acid	Caffeic Acid	Cinnamic Acid	
		4-hydroxy-3,5-dimethoxybenzoic acid	Syringic Acid	Dimexthoxybenzene	(Wolf et al., 2018)
		(1*S*,4*aS*,7*R*,7*aS*)-7-hydroxy-7-(hydroxymethyl)-1-[(2*S*,3*R*,4*S*,5*S*,6*R*)-3,4,5-trihydroxy-6	Monotropein	Iridoid	
		(1*S*,4*aS*,5*S*,7*aS*)-5-hydroxy-7-(hydroxymethyl)-1-[(2*S*,3*R*,4*S*,5*S*,6*R*)-3,4,5-trihydroxy-6	10-deacetylasperulosidic acid	Iridoid	(Wolff et al., 2019)
F. hyacinthina	Leaf (MeOH extract)	(2S)-isosakuranetin-7-*O*-ß-D-apiofuranosyl-(1→6)-ß-D-glucopyranoside	4'Me naringenin	Flavanone	
		5,3',5'-trihydroxy-flavanone-7-*O*-ß-D-apiofuranosyl-(1→6)-ß-D-glucopyranoside		Flavanone	
		naringenin-7-*O*-ß-D-apiofuranosyl-(1→6)-ß-D-glucopyranoside		Flavanone	
		quercetin-4'-ß-D-*O*-glucopyranosyl-3-*O*-rutinoside		Flavanol	
		2-(3,4-dihydroxyphenyl)-5,7-dihydroxy-3-[(2S,3R,4S,5S,6R)-3,4,5-trihydroxy-6-[[(2R,3R,	Rutin	Flavanol	(Barboza et al., 2018)
		(*E*)-3-(3,4-dihydroxyphenyl)prop-2-enoic acid	Caffeic Acid	Cinnamic Acid	
		4-hydroxy-3,5-dimethoxybenzoic acid	Syringic Acid	Dimexthoxybenzene	
		7-hydroxy-6-methoxychromen-2-one	Scopoletin	Hydroxycoumarin	(Wolf et al., 2018)
		(1*S*,4*aS*,7*R*,7*aS*)-7-hydroxy-7-(hydroxymethyl)-1-[(2*S*,3*R*,4*S*,5*S*,6*R*)-3,4,5-trihydroxy-6	Monotropein	Iridoid	
		methyl (1*S*,4*aS*,7*R*,7*aS*)-7-hydroxy-7-(hydroxymethyl)-1-[(2*S*,3*R*,4*S*,5*S*,6*R*)-3,4,5-trihy	Monotropein methyl ester	Iridoid	
		(1*S*,4*aS*,5*S*,7*aS*)-5-hydroxy-7-(hydroxymethyl)-1-[(2*S*,3*R*,4*S*,5*S*,6*R*)-3,4,5-trihydroxy-6	10-deacetylasperulosidic acid	Iridoid	(Wolff et al., 2019)
F. truncata	Leaves (MeOH extract)	(2S)-isosakuranetin-7-*O*-ß-D-apiofuranosyl-(1→6)-ß-D-glucopyranoside	4'Me naringenin	Flavanone	
		narigenin-7-*O*-ß-D-apiofuranosyl-(1→6)-ß-D-glucopyranoside		Flavanone	
		kaempferol-3-*O*-rutinoside		Flavanol	
		1-[4-[(2S,3R,4S,5S,6R)-6-[[(2R,3R,4R)-3,4-dihydroxy-4-(hydroxymethyl)oxolan-2-yl]oxy	Erythroxyloside A	Acetophenone glycoside	
		[(4S,7S,8S,11S)-2-oxo-8-[(2S,3R,4S,5S,6R)-3,4,5-trihydroxy-6-(hydroxymethyl)oxan-2-yl	Asperuloside	Iridoid glycoside	(Barboza et al., 2018)
		4-hydroxy-3,5-dimethoxybenzoic acid	Syringic Acid	Dimexthoxybenzene	
		7-hydroxy-6-methoxychromen-2-one	Scopoletin	Hydroxycoumarin	(Wolf et al., 2018)
		(1*S*,4*aS*,5*S*,7*aS*)-5-hydroxy-7-(hydroxymethyl)-1-[(2*S*,3*R*,4*S*,5*S*,6*R*)-3,4,5-trihydroxy-6	10-deacetylasperulosidic acid	Iridoid	(Wolff et al., 2019)

2.0 Materials and methods

2.1 Analytical methods

Two analytical methods were used to verify the purity of extracted compounds and help in the decision making of purifying and identifying compounds throughout this experiment.

2.1.1 Thin layer chromatography (TLC)

Aluminum-backed silica gel 60 TLC plates were used to verify the purity of extractions, compare newly extracted compounds to already-known substances, and to identify potentially interesting fractions in a series. 5–20 µL of each sample were transferred to the plates via glass capillaries until spots were present under UV-light at 254 nm. Different solvent mixtures were used throughout the study for plate development and depended upon the polarity of the target compounds. The most lipophilic compounds travelled farthest and were found near the top of the plates, so the goal for each plate was to spread the more polar compounds evenly without pushing the most lipophilic off. The plates contained green fluorescence indicator and were therefore checked under UV light at 254 nm; dark spots caused by fluorescence quenching showed the locations of some transferred compounds and could be used to infer retention factors and relative concentrations. Plates were also observed under UV light at 366 nm, where the fluorescence of the compound itself could be seen, this occasionally gave hints about the class of compounds the substance might contain. In this work, solvent mixtures based on chloroform ($CHCl_3$) and methanol in the ratios 98:2 and 80:20 were used. To detect compounds that are not UV active, the anisaldehyde reagent was chosen to obtain visible spots after heating the plate. The Dragendorff's reagent was used to detect alkaloids in the crude extract and Naturstoffreagenz A (1% in methanol) was used to detect flavonoids.

2.1.2 High performance liquid chromatography (HPLC)

HPLC was used many times throughout the isolation process to gain information about the compounds within each sample. This type of chromatography takes a small amount of sample and pumps different compositions of the eluents under high pressure through a reverse phase silica gel column to separate individual constituents. The stronger affinity for the mobile phase a constituent has, the faster it will move through the column, and the stronger affinity for the stationary phase, the slower; in this case, the more lipophilic compounds took the longest time to elute.

Hypersil BDS C-18 (250 × 4.6 mm; 5 µm particle size, for a flow rate of 1.0 mL/min) and Hypersil BDS-C18 (100 × 4.0 mm; 3 µm particle size, for a flow rate of 0.5 mL/min) were used as stationary phases; solvent mixtures changed according to the polarity of the target compound, these methods are described in Table 2. Detection usually occurred via a UV-Vis diode array detector at 230 nm, where most compounds show absorbance, but occasionally further investigation at other wavelengths was necessary. The retention time and UV-spectrum provided a "fingerprint" of each constituent, which could then be compared to the in-house database of known compounds for identification. Unknown compounds were checked for purity and sent to the NMR facilities at the University of Vienna Department of Chemistry for further identification.

Table 2: Solvent mixtures for HPLC measurements. A= 10 mM aqueous ammonium acetate solution and B= methanol.

Time [min]	A [%]	B [%]	Flow [mL/min]	Max Pressure Limit [bar]
0.00	80.0	20.0	1.000	--
15.00	10.0	90.0	1.000	--
15.10	1.0	99.0	1.000	--
22.00	1.0	99.0	1.000	--

Time [min]	A [%]	B [%]	Flow [mL/min]	Max Pressure Limit [bar]
0.00	97.5	2.5	0.500	--
12.00	75.0	25.0	0.500	--
12.10	2.5	97.5	0.500	--
15.00	2.5	97.5	0.500	--

Time [min]	A [%]	B [%]	Flow [mL/min]	Max Pressure Limit [bar]
0.00	95.0	5.0	0.500	--
2.00	95.0	5.0	0.500	--
2.10	60.0	40.0	0.500	--
11.00	5.0	95.0	0.500	--
15.00	5.0	95.0	0.500	--

Time [min]	A [%]	B [%]	Flow [mL/min]	Max Pressure Limit [bar]
0.00	80.0	20.0	0.500	--
4.40	28.7	71.3	0.500	--
4.44	1.0	99.0	0.500	--
10.00	1.0	99.0	0.500	--

2.2 Preparative methods

2.2.1 Sample collection

The *F. tamberlikiana* collection took place in Costa Rica at the Tropical Field Station of the University of Vienna in 2016.

2.2.2 Extraction process

Five bags of sample were obtained with the masses given in Table 3. Each bag of sample was processed separately to allow for later comparison of compounds, the following steps took place for each. Dry leaf material was macerated using a blender then placed into a vessel with an excess of MeOH. The mixture was sonicated in an ultrasonic bath for twenty minutes, then the liquid was removed from the leaf material via a filter funnel. The resulting solution was placed on a rotary evaporator in a water bath not exceeding 40°C to avoid degradation of compounds. The MeOH collected from the receiving flask was then poured into the leaf material, ultrasonicated, and the process was repeated three more times. After this process was completed for all samples the following crude extract masses were obtained and recorded in Table 3B.

Table 3: Dry weights of leaf material from each sample bag (left). Weights of crude extracts after initial methanol extraction (right).

Sample	Weight (g)
1	58.9
2	60.6
3	70.4
4	54.0
5	60.2

Sample	Weight(g)
1	1.0
2	1.1
3	2.0
4	1.1
5	1.7

2.2.3 Liquid-liquid extraction

Liquid-liquid extraction was performed on the crude extract of each sample separately in order to roughly separate their constituents according to solubility and polarity. This technique relies on the different solubilities of compounds in immiscible solvents. First, the crude extract from sample 1 was suspended in $CHCl_3$ and placed in a separation funnel, then a roughly equal amount of H_2O (approx. 50 mL) was added. The funnel was shaken, allowed to settle, and the organic layer was drained from the water into a round-bottom flask. More $CHCl_3$ was added to flush the water layer of remaining lipophilic substances, then was once again drained into the round-bottom flask. This process was repeated two additional times until the $CHCl_3$ ran mostly clear. The same steps were taken to yield an intermediary polar phase using EtOAc as the solvent. At the end of the liquid-liquid extractions, three crude extracts were obtained: H_2O-, ethyl acetate (EtOAc)-, and $CHCl_3$-phases. The same procedure took place for the crude extract of samples 1–5. After examination via HPLC measurements, the five crude extracts for each phase were then pooled together.

2.2.4 Column chromatography of the ethyl acetate phase

The ethyl acetate extract obtained was separated into fractions via silica gel column chromatography. Once again, this separation occurred by manipulation of the polarity of the mobile phase; a slurry using *n*-heptane and 20 g of silica gel 60 (0.2–0.5 mm particle size) was poured into a glass column with cotton at the bottom and allowed to settle. Three grams of silica gel was added to a mortar and pestle, then 210 mg of the EtOAc extract was adsorbed on this silica gel. The solvent was allowed to evaporate, and the dry mixture was then transferred to the column and topped with sand. Nonpolar compounds move down the column more quickly, while polar substances

adhere to the stationary phase for longer as the ratios of solvents change. The different speeds at which different molecules move allow the constituents within the EtOAc extract to separate. The column was eluted with 100mL of the solvent mixtures listed in Table 4, and 50 mL fractions were collected in flasks labelled I/1, I/2 through XIII/1.

Table 4: Column solvent mixtures for the ethyl acetate extract separation.

Solvent	*n*-Heptane (mL)	EtOAc (mL)	Solvent	MeOH (mL)	EtOAc (mL)
I	100	0	XII	20	80
II	80	20	XIII	50	50
III	80	20			
IV	70	30			
V	60	40			
VI	50	50			
VII	40	60			
VIII	30	70			
IX	20	80			
X	10	90			
XI	0	100			

2.2.5 Column chromatography of the water phase

In much the same way, the water extract was separated into fractions via silica gel column chromatography. A slurry was made using PE and 25 g of silica gel 60 (0.2-0.5 mm particle size) and poured into a glass column. 3.5 g of the H_2O extract was transferred onto 2 g of silica gel and the dry mixture was added to the column and topped with sand. The column was eluted with 100 mL of the solvent mixtures listed in Table 5, and 50 mL fractions were collected in flasks labelled I/1, I/2 through VIII/1, VIII/2.

Table 5: Column solvent mixtures for water extract separation.

Solvent	PE (mL)	EtOAc (mL)
I	80	20
II	50	50
III	25	75
IV	0	100
Solvent	MeOH (mL)	EtOAc (mL)
V	10	90
VI	25	75
VII	50	50
VIII	100	0

Separation via size-exclusion chromatography

Size-exclusion chromatography was performed several times throughout the duration of this experiment to obtain further purification of the column fractions. Sephadex LH20 is a gel-like substance made of cross-linked dextran beads with pores of controlled sizes. When a mixture of molecules is passed through a Sephadex LH20 column, smaller molecules move more slowly through the column because they enter the pores of the gel beads, resulting in a longer path to travel. Larger molecules, unable to enter the smaller pores, move more quickly through the column since they follow a more direct route around the silica beads. In this way, the Sephadex LH20 column works to separate similarly polar molecules according to their hydrodynamic volume for further purification. A pre-filled column was used with SephadexLH20 and the mobile phase was MeOH. Concentrated samples of the column fractions were pipetted on top of the Sephadex LH20 gel and MeOH was added to develop. The resulting subfractions were collected in 10 mL flasks.

2.2.6 Preparative thin layer chromatography (pTLC)

Preparative TLC plates were used as a final purification step several times throughout the duration of the experiment. To do this, the samples were applied in a line 1 cm above the bottom edge of a glass-backed plate with silica gel 60 (0.5 mm thickness). The plate was developed in a solvent mixture depending on the polarity of the target compound. The separation was then checked under UV light and the bands were marked with pencil. The bands were then scraped off the plate and deposited into separate flasks and covered with MeOH to avoid oxidation. The flasks were then placed in an ultrasonic bath to extract the sample from the silica gel, then filtered under vacuum pressure to remove the silica. Purity was checked via TLC and HPLC and dry mass was recorded.

2.2.7 Nuclear magnetic resonance spectroscopy (NMR) and mass spectrometry (MS)

Purified samples were sent for structure elucidation to the Institute for Organic Chemistry at the University of Vienna. The dried samples were dissolved in 0.7 mL CD_3OD and analyzed using a Bruker Avance III 600 spectrometer operating at 600.13

MHz (1H) or 150.61 MHz (13C), with data processing performed via Topspin 3.5 software. Mass spectra were obtained on a high-resolution time-of-flight (HR-TOF) mass spectrometer (maXis, Bruker Daltonics, Billerica, MA, USA) via direct infusion electrospray ionization (ESI) in both positive ionization mode (mass accuracy within 5 ppm) and negative ionization mode (mass accuracy within 10 ppm) based on the protocol by Kornpointer et al. (2022).

2.2.8 Insect Assay

For this assay, third instar larvae of the cotton leaf worm *Spodoptera littoralis* Boisduval. were used (CABI, 2022). The aim of this experiment was to infer the taste of the phenylpropanoid eugenol and its glycosylated derivatives. This protocol was based on a 2002 study from Glendinning et al., where *Manduca sexta* was used to infer generalist response to bitter tasting plant material using caffeine, salicin, and aristolochic acid. As both insect species are generalist agricultural pests and members of the order *Lepidoptera*, it is assumed that *S. littoralis* will show a similar aversion to these three bitter compounds. Additionally, previous studies have shown that caffeine has adverse impacts on *S. littoralis* (Seada et al., 2018) and both salicin and aristolochic acid have been posited as organic insecticides against *Spodoptera* due to the antifeedant activity they induce (Baskar et al., 2011; Hussein et al., 2023). By comparing eugenol and its related compounds with known bitter compounds, it can be determined whether eugenol derivatives provide leaf tissue with similar protection from herbivory.

Spodoptera littoralis larvae (at a length of 10–15 mm) were obtained from the existing population at the University of Vienna, Department of Botany and Biodiversity. Individuals which showed signs of preparation for skin shedding were avoided. The larvae were collected and left in the dark to hunger overnight. For each leaf disk, approximately 20 µL of solution were used. Several controls were used to obtain results that provide the most accurate picture of feeding activity possible. These controls included:

- A wilting control with no solution to account for potential water loss over time.

- A lettuce control without additional solution: blank leaf disks used to track caterpillar feeding response to plain lettuce.
- A control with an 80:20 water-to-acetone solution dispersed onto the leaf disks; this was included to track any adverse response the larvae might have due to the solution all compounds were dissolved in.
- The three control compounds which act as a comparison for bitter taste according to Glendinning et al. (2002): salicin, caffeine, or aristolochic acid. All were set to a 2.5 mg/mL concentration.

The two eugenol derivatives purified from *F. tamberlikiana* leaf extractions were used: hydroxychavicol (**1**), and 2-methoxy-4-(2-propen-1-yl)phenyl-6-*O*-D-apio-β-D-furanosyl-β-D-glucopyranoside (**2**), as well as a eugenol stock solution. These three compounds were diluted to the concentrations of 2.5, 1.25, and 0.625 mg/mL. One 1.3 cm leaf disk was placed in a 5.5 cm petri dish on top of moistened filter paper alongside one *S. littoralis* larva. Three replicates were performed per treatment, as well as for each control, and photos were taken at the 15, 30, 40, and 60-minute marks. Leaf area assessment was performed using Imagej 1.54k software.

3.0 Results and Discussion

In this study, compounds **1**-**7** (Figure 10) belonging to phenylpropanoids (**1**, **2**, **3**), terpenoids (**4**, **5**), flavonoids (**6**) and benzoic acid derivatives (**7**) were purified from the investigated plant sources collected in Costa Rica in 2016. In collaboration with the Department of Organic Chemistry at the University of Vienna, these compounds were identified through structural elucidation techniques, including nuclear magnetic resonance (NMR) spectroscopy and mass spectrometry (MS). The identified structures (Figure 10) revealed two key biosynthetic pathways of particular significance: the phenylpropanoid and terpenoid pathways. Among the major isolated phenylpropanoids, their herbivory-deterrent activity was evaluated and compared against the commercially available compound eugenol, providing insights into their potential ecological roles and bioactive properties. This comparative analysis highlights the functional relevance of these metabolites as well as their potential impact on generalist herbivores.

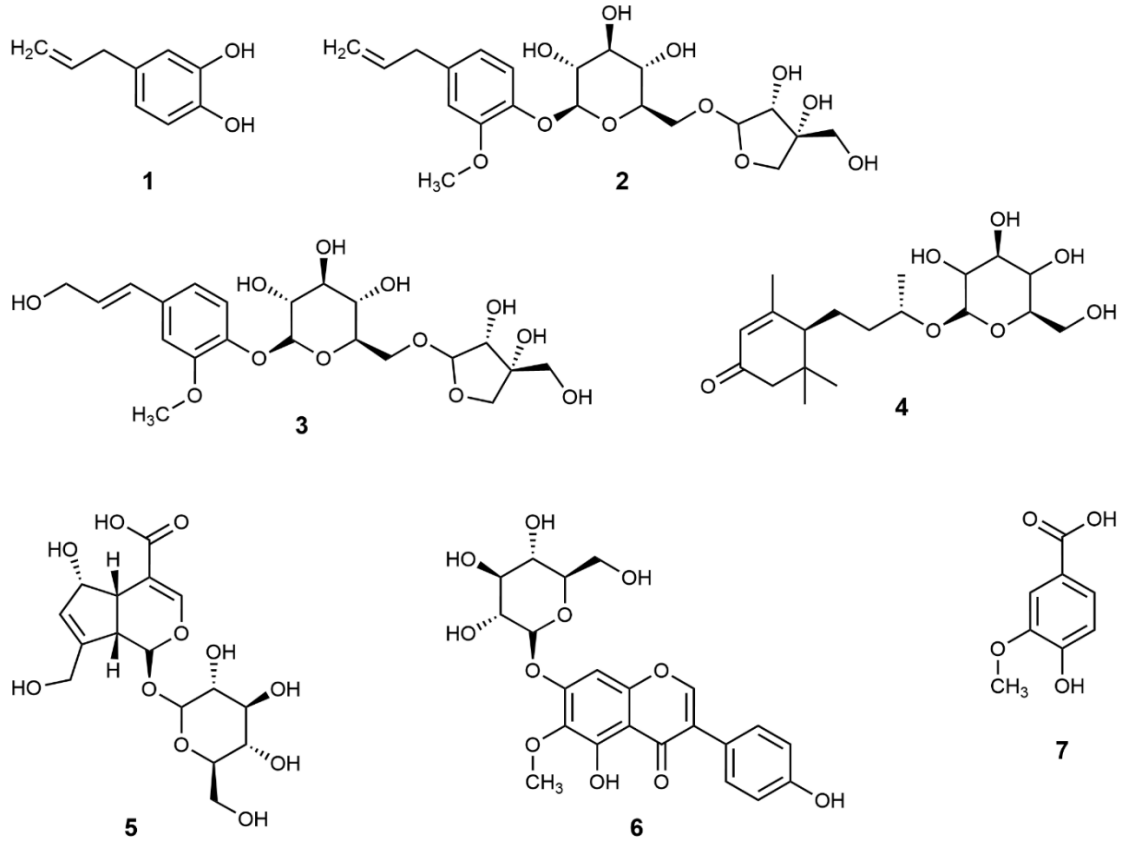

Figure 10: Chemical structures of the isolated compounds: hydroxychavicol (**1**), the eugenol-1-*O*-glycoside 2-methoxy-4-(2-propen-1-yl)phenyl-6-*O*-D-apio-β-D-furanosyl-β-D-glucopyranoside (**2**), ligusinenoside A (**3**), blumenol C glucoside (**4**), deacetylasperulosidic acid (**5**), tectoridin (**6**), vanillic acid (**7**).

The compounds depicted in Figure 10 are organized according to their prevalence in the phytochemical profile of *F. tamberlikiana*. As illustrated in Figure 11, the eugenol-derivative, 2-methoxy-4-(2-propen-1-yl)phenyl-6-*O*-D-apio-β-D-furanosyl-β-D-glucopyranoside (**2**), is the most dominant component of the crude extract. Ligusinenoside A (**3**) is the next most prominent isolated compound, followed by hydroxychavicol (**1**). Figure 11 highlights the significant presence of phenylpropanoids, which constitute the majority of metabolites accumulated in the dried plant material.

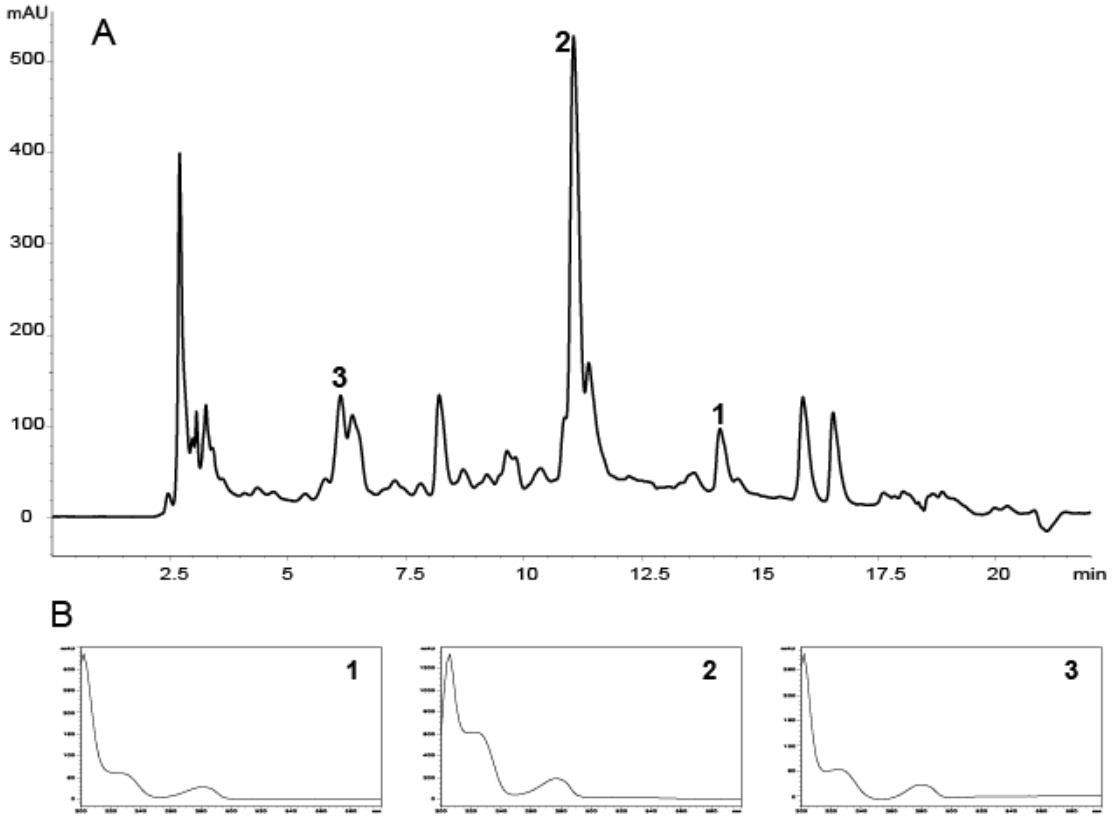

Figure 11: The HPLC profile of the investigated crude methanolic extract (A) with the identified phenylpropanoids: hydroxychavicol (**1**), 2-methoxy-4-(2-propen-1-yl)phenyl-6-*O*-D-apio-β-D-furanosyl-β-D-glucopyranoside (**2**) and Ligusinenoside A (**3**). UV spectra of these phenylpropanoids (B). The peaks of the other identified compounds are hidden in the not well separated peaks.

3.1 Phenylpropanoids

Phenylpropanoids represent the most abundant class of phytochemicals in *F. tamberlikiana*, both in terms of the number of isolated compounds and their overall relative quantity (Figure 11). This observation is consistent with previous research, which also identified phenolics as one of two major classes of specialized metabolites

in the *Faramea* genus (Table 1). The dominance of phenylpropanoids in *Faramea tamberlikiana* further highlights the importance of phenolic pathways in shaping the chemical ecology of the *Faramea* genus.

Moreover, these findings underscore the necessity of understanding the ecological roles and functions of phenylpropanoids in the environment. As the most prevalent compounds throughout the plant's tissues (Figure 11), these compounds exert important effects on surrounding organisms. Previous studies have indicated that these compounds contribute to various ecological interactions: in leaf tissues, they may act as anti-herbivory defenses or attraction compounds for certain specialized bee species (Naoumkina et al., 2010; Rocha-Filho and Garófalo, 2013) In addition to their potential roles in deterring herbivores, phenylpropanoids can also serve as signaling molecules, as scents that attract beneficial pollinators or microbial partners in roots (Naoumkina et al., 2010). Therefore, elucidating the ecological significance of these abundant metabolites is crucial for understanding the broader ecological dynamics within the habitats of *Faramea tamberlikiana* as well as the genus at large.

3.1.1 Phenylpropanoid Derivatives

In this study, two phenylpropanoid derivatives—hydroxychavicol (**1**) and the eugenol-derivative, named 2-methoxy-4-(2-propen-1-yl)phenyl-6-*O*-D-apio-β-D-furanosyl-β-D-glucopyranoside (**2**)—were isolated from the ethyl acetate phase and ligusinenoside A (**3**) was isolated from the water phase of *F. tamberlikiana*. These compounds appear to be the most significant compounds isolated and may play a defining role in the chemical ecology of *F. tamberlikiana*. The characteristic fragrance of the plant, attributed to these aromatic compounds, was noticeable throughout the study, and eugenol derivatives were found in the leaves, indicating a broader ecological function beyond floral scent. In addition to their potential role in herbivore deterrence and microbial defense, phenolics such as eugenol are known attractants for male euglossine (orchid) bees, which collect these volatiles as part of their mating displays (Rocha-Filho and Garófalo, 2013). Further field research could help clarify the ecological functions of these cinnamic acid derivatives in both plant defense and insect interactions.

*3.1.1.1 Hydroxychavicol (**1**), 2-methoxy-4-(2-propen-1-yl)phenyl-6-O-D-apio-β-D-furanosyl-β-D-glucopyranoside (**2**) and Ligusinenoside A (**3**)*

The phenylpropanoid derivatives hydroxychavicol (1) and 2-methoxy-4-(2-propen-1-yl)phenyl-6-O-d-apio-β-d-furanosyl-β-d-glucopyranoside (2) are both are derived from cinnamic acid and related to eugenol, an aromatic phenolic compound well known for its prominence in the scent and spice of cloves (Syzygium aromaticum, (L.) Merr. & L.M.Perry Myrtaceae). Throughout the research, the plant material and extracts maintained their characteristic fragrance, attributed to these aromatic compounds. The presence of these derivatives seems to act as a defining characteristic of F. tamberlikiana, as the compounds are present not only in the flowers but throughout the leaf tissues, making the plant easily recognizable in the field. These types of phenolic compounds are often produced by plants to deter herbivores and protect against pathogenic microbes (Tan and Nishida, 2012). Further investigation aimed to determine whether these cinnamic acid derivatives provided antifeedant protection for *F. tamberlikiana*.

Because hydroxychavicol (**1**) and 2-methoxy-4-(2-propen-1-yl)phenyl-6-*O*-D-apio-β-D-furanosyl-β-D-glucopyranoside (**2**) are structurally similar to eugenol, it is reasonable to infer that these compounds might exhibit similar biological activities to those known for eugenol. While eugenol has a methoxy group at the position C-2, hydroxychavicol (**1**) has a hydroxyl group at the same position and the glycosylated eugenol derivative (**2**) shares the eugenol backbone and has an attached glucose molecule (see section 1.2.4.2 Coniferyl Alcohol and Eugenol). One well-known ecological role of eugenol is its ability to attract certain species of South American male euglossine (orchid) bees (Rocha-Filho and Garófalo, 2013). These bees collect volatile compounds like eugenol from various plant parts to create a scent-blend as part of their courtship displays in order to attract mates (Rocha-Filho and Garófalo, 2013). Since the eugenol compounds in *F. tamberlikiana* are concentrated in the leaves rather than the flowers, they could potentially serve a role beyond pollination, which suggests they may play a specialized part in scent collection by orchid bees, rather than serving a purely reproductive function. Further field study would be required to determine whether this is the case.

Ligusinenoside A (**3**), a phenylpropanoid diglycoside, was isolated from the water phase. This compound was previously identified in the rhizome of *Ligusticum sinensis* Oliv. in the *Apiaceae* family (Ma et al., 2007). Ligusinenoside A (**3**) is a type of coniferyl alcohol, a key intermediate of both lignin and eugenol synthesis (Metsämuuronen and Sirén, 2019; Koeduka et al., 2006). Given the abundance of eugenol-related compounds, it is possible that this compound serves as a precursor to eugenol-related biosynthetic pathways (Metsämuuronen and Sirén, 2019). Further study would be required to clarify its exact role in the plant's metabolic network.

3.2 Megastigmanes and Iridoids

This study identified one apocarotenoid megastigmane, blumenol C glucoside (**4**), and the iridoid deacetylasperulosidic acid (**5**) in the leaf tissues of *F. tamberlikiana*. Blumenol C glucoside was isolated from the lipophilic part of the crude extract. Megastigmanes are a subclass of apocarotenoids, which are oxidative cleavage products of carotenoids and play a critical role in plant signalling and symbiotic relationships (Hou et al., 2016). The identification of blumenol C glucoside (**4**) in *F. tamberlikiana* offers insights into the plant's nutrient acquisition strategies, particularly its interaction with arbuscular mycorrhizal fungi. These fungi are known to enhance phosphorus uptake, a critical adaptation for plants growing in nutrient-poor soils, such as those in the native habitat of *F. tamberlikiana* (Hou et al., 2016).

3.2.1 Blumenol C Glucoside (**4**) and Deacetylasperulosidic acid (**5**)

Blumenol C glucoside (**4**) is a type of carotenoid compound isolated from the lipophilic part of the crude methanolic extract. More specifically, blumenol is an apocarotenoid, or a compound formed through the oxidative cleavage of carotenoids, which most often functions in plant signaling (Wang et al., 2018; Hou et al., 2016). While carotenoids tend to be larger compounds related to pigmentation, apocarotenoids are smaller, more easily soluble, and more volatile (Wang et al., 2018).

Blumenols are grouped into three different types: blumenol A, blumenol B, and blumenol C, based on conformational changes to the core molecular structure (Wang et al., 2018). These compounds belong to megastigmanes, a class of oxygenated

isonorterpenoids with a C_{13} carbon skeleton (Kornpointner et al., 2022). These compounds are prone to structural changes, particularly in the position of oxygen atoms, due to the instability of their conjugated double bonds (Kornpointner et al., 2022). As a result, blumenol is prone to glycosylation, or the addition of a sugar molecule, which reduces reactivity, as was the case for the blumenol C glucoside (**4**) found in this study (Hou et al., 2016). Interestingly, blumenol C derivatives in particular have been shown to play a role in signalling arbuscular mycorrhizal fungi (Wang et al., 2018). This is significant because these fungi form a symbiotic relationship with plants, and facilitate mineral nutrient uptake, especially that of phosphorus (Wang et al., 2018). The presence of blumenol C glucoside (**4**) in *F. tamberlikiana* provides insight into the ways in which the species manages nutrient acquisition in the nutrient-poor soils in its native range.

Iridoids are one of the most important classes of compounds found in the genus *Faramea*, as shown in Table 1. In particular, deacetylasperulosidic acid (**5**) was found in three other species: *F. bahiensis*, *F. hyacynthina*, and *F. truncata* (Barboza et al., 2018; Wolff et al., 2018; Wolff et al., 2019). Deacetylasperulosidic acid (**5**) is a bitter-tasting compound thought to play a role in herbivory deterrence but has also been shown to exhibit antiviral and antimicrobial properties (Barboza et al., 2018). Both deacetylasperulosidic acid (**5**) and asperuloside are considered hallmark compounds that are found in all *Rubioideae* subfamily members (Wolff et al., 2019). Although the identification of deacetylasperulosidic acid (**5**) in this study further supports the idea that iridoids are an important class of compounds within the genus, and may someday prove to be chemotaxonomically important, only one iridoid compound was identified. This may be due to the limitations of this study. Several iridoid glucosides were identified in a 2019 study in the stems of *F. bahiensis*, *F. hyacynthina*, and *F. truncata*, including monotropein and monotropein methyl ester (Wolff et al., 2019). Because of the glucose moiety in these compounds, they are relatively polar and would likely be found solvated in water. In this study, due to the polarities of the compounds involved in the water phase, not all were successfully separated from one another to allow for identification. Therefore, it is possible that some iridoids were left unidentified and further study using different separation techniques would be necessary to ensure no

iridoid compounds remain. It is also just as plausible that, in *F. tamberlikiana*, iridoid compounds play only a minor role in the phytochemical profile.

3.3 Isoflavonoids

One isoflavone, tectoridin (**6**), was successfully isolated from the lipophilic phase of *F. tamberlikiana* in this study. Isoflavones, typically found in leguminous plants, are biosynthesized via the isoflavone biosynthetic pathway, which originates from the phenylpropanoid pathway. Although the specific biosynthetic route in *F. tamberlikiana* remains uncertain, the presence of tectoridin (**6**) highlights the potential ecological and pharmacological roles of isoflavonoids in this species, possibly linked to defense mechanisms or symbiotic interactions.

3.3.1 Tectoridin (**6**)

Tectoridin (**6**) is an isoflavone and was purified from the lipophilic phase column. The isoflavone biosynthetic pathway is distributed mainly, though not exclusively, in leguminous plants where these compounds often play a key role in symbiotic relationships, such as attracting nitrogen-fixing bacteria (Liu et al., 2021). Isoflavonoids, in general, are distributed across various plant families and have been previously isolated in at least two *Rubiaceae* family members (Lapčík, 2007; Lu et al., 2014). However, prior to this study, no isoflavonoids were reported from any member of the *Faramea* genus, making it a novel finding, which reflects a broader trend of rare isoflavonoid occurrence in non-leguminous plants.

Further, in a 2023 published study of the role of tectoridin (**6**) and its derivatives in *Belamcanda chinensis* L., it was found that these isoflavonoids play crucial roles in plant defense. The compounds displayed both herbivory-deterrent and antipathogenic activities (Cheng et al., 2023). This evidence suggests that the presence of tectoridin in *F. tamberlikiana* might serve similar defensive functions in helping protect the plant from microbial infections and insect threats. This aligns with the established ecological roles of isoflavonoids as chemical defenses in a wide range of plant species, but further study would be needed to determine whether this is the case.

3.4 Benzoic acids

One benzoic acid was isolated from multiple fractions of both the water and ethyl acetate phases in *F. tamberlikiana*: vanillic acid (7). This phenylpropanoid compound can be biosynthesized through a variety of different pathways. Known for its role as a flavoring agent, vanillic acid (7) is also recognized for attracting male orchid bees, which collect it for mating displays. In *F. tamberlikiana*, the presence of vanillic acid (7), alongside abundant eugenol derivatives, suggests its ecological significance, potentially enhancing the plant's attractiveness to scent-collecting bees while possibly playing a defensive role by deterring herbivores due to its strong odor and taste.

3.4.1 Vanillic Acid (7)

Vanillic acid (7) is a phenylpropanoid compound found in several fractions throughout both the water and ethyl acetate phases. Vanillic acid can be synthesized in a variety of different ways. In one case, the starting material for vanillic acid is benzoic acid derived from the chlorismate of the phenylpropanoid pathway (Vogt, 2010). Benzoic acid undergoes transformation to protocatechuic acid and eventually to vanillic acid (7) (Metsämuuronen and Sirén, 2019). Vanillic acid (7) can also be synthesized through the degradation of lignin; in this case, ferulic acid is the substrate and the compound is transformed to feruloyl CoA, then vanillin, and finally vanillic acid (7) (Metsämuuronen and Sirén, 2019). In either case, vanillic acid (7) could result as a relic of the degradation of the other phenylpropanoids discussed.

Vanillic acid (7) is most commonly known as a flavoring agent, but it is also effective in attracting male orchid bees (Rocha-Filho and Garófalo, 2013). This, combined with its abundant cinnamic acid derivatives may make the leaves of *F. tamberlikiana* attractive for scent collection. Further, vanillic acid (7) may demonstrate antifeeding activity, as its strong smell and taste is likely unattractive to herbivores.

3.5 Insect Assay

Based on compound extractions and comparison with HPLC and NMR data, it was shown that the major substances contained within the leaves of *F. tamberlikiana* are

2-methoxy-4-(2-propen-1-yl)phenyl-6-*O*-D-apio-β-D-furanosyl-β-D-glucopyranoside (**2**) and its related compounds. For this reason, these compounds were further investigated to obtain a better understanding of their potential function. Anecdotally, both the fresh leaf material and subsequent extractions smelled strongly of eugenol, a related compound, and the HPLC comparison of crude extract and compound data showed that these compounds were produced in tissue abundantly Figure 11. Therefore, a well-rounded understanding of the potential uses of this compound is crucial in understanding its role in *F. tamberlikiana*, as well as its broader ecological implications in the surrounding ecosystem.

An insect assay was performed to gain insight into the impact of these compounds on the feeding behavior of a generalist herbivore, *Spodoptera littoralis*. This insect species was chosen as it is a highly polyphagous herbivore that is one of the most devastating agricultural pests worldwide, particularly in the tropics and subtropics (Hosseini, 2023). In its larval stage, *S. littoralis* is known for its voracious appetite and ability to feed on a wide range of unrelated plant species, thus it is often used in scientific research as a proxy for local generalist herbivores.

Eugenol was selected for comparison with hydroxychavicol (**1**) and 2-methoxy-4-(2-propen-1-yl)phenyl-6-*O*-D-apio-β-D-furanosyl-β-D-glucopyranoside (**2**) because all three compounds possess similar core structures. Eugenol is known for its strong taste and scent, which is typically avoided by generalist herbivores, and was therefore used as a comparison to determine whether the other two compounds exhibit similar antifeeding activity. The most prominent compound in the chemical profile, 2-methoxy-4-(2-propen-1-yl)phenyl-6-*O*-D-apio-β-D-furanosyl-β-D-glucopyranoside (**2**), is a glycosylated eugenol derivative with an attached sugar moiety. This glucose addition enhances the solubility of the molecule and facilitates storage within plant tissues without altering the core molecular structure. Sugar moieties are often cleaved upon insect attack, whether through enzymatic activity in the saliva or gut of herbivores, allowing the active portion of the molecule to exert its effects.

Figure 12 depicts the remaining areas of leaf disks treated with three bitter taste controls salicin, caffeine, and aristolochic acid as well as the eugenol stock solution, with all compounds at a concentration of 2.5 mg/mL (Glendinning et al., 2002). This comparison aimed to assess whether eugenol has a similar effect to known bitter

compounds on the feeding rate of *S. littoralis*, and if so, whether it can be classified as a bitter or otherwise feeding-deterrent compound. The results show that eugenol and its derivatives significantly outperform aristolochic acid in deterring feeding. Moreover, eugenol exhibits a deterrent effect comparable to salicin. Based on these findings, eugenol appears to exhibit bitter-tasting activity in *S. littoralis* and may offer similar protection against generalist herbivores as salicin and caffeine. Because eugenol, in contrast to 2-methoxy-4-(2-propen-1-yl)phenyl-6-*O*-D-apio-β-D-furanosyl-β-D-glucopyranoside (**2**), is a volatile compound, the deterring effect may also come from its released vapors. It can be inferred that eugenol, related to the most abundant derivatives found in *F. tamberlikiana*, is perceived as similarly bitter by *Spodoptera littoralis* larvae to known bitter compounds.

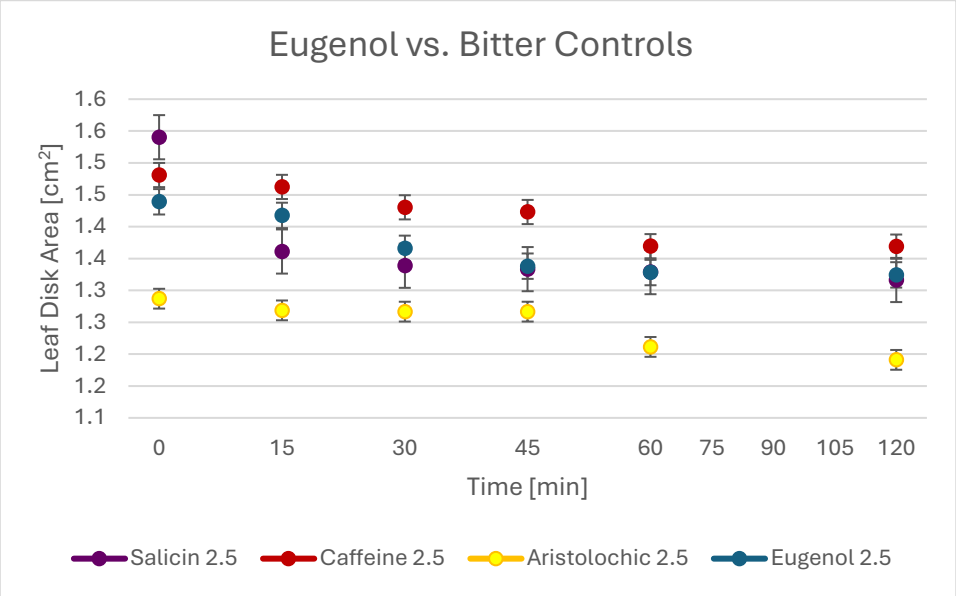

Figure 12: Comparison of the remaining areas of leaf disks after feeding by *S. littoralis* over a period of 120 minutes. Leaf disks had different bitter compounds salicin, caffeine, and aristolochic acid or a eugenol stock solution dispersed onto them prior to feeding. All compounds were set to a concentration of 2.5 mg/mL.

Figure 13 illustrates whether eugenol affects feeding behavior compared to control plant material. A stock solution of eugenol at 2.5 mg/mL was used and compared with both plain lettuce and leaf disks treated with an 80:20 water/acetone solution. The feeding rates for both negative controls appear nearly identical, suggesting that the water/acetone solution has minimal impact on the insects' feeding behavior. Therefore, any observed changes in feeding can be attributed primarily to the compounds themselves rather than the solvent. Notably, eugenol demonstrates a

significant reduction in feeding compared to the control plant material, indicating its potential role as an anti-herbivory defense compound.

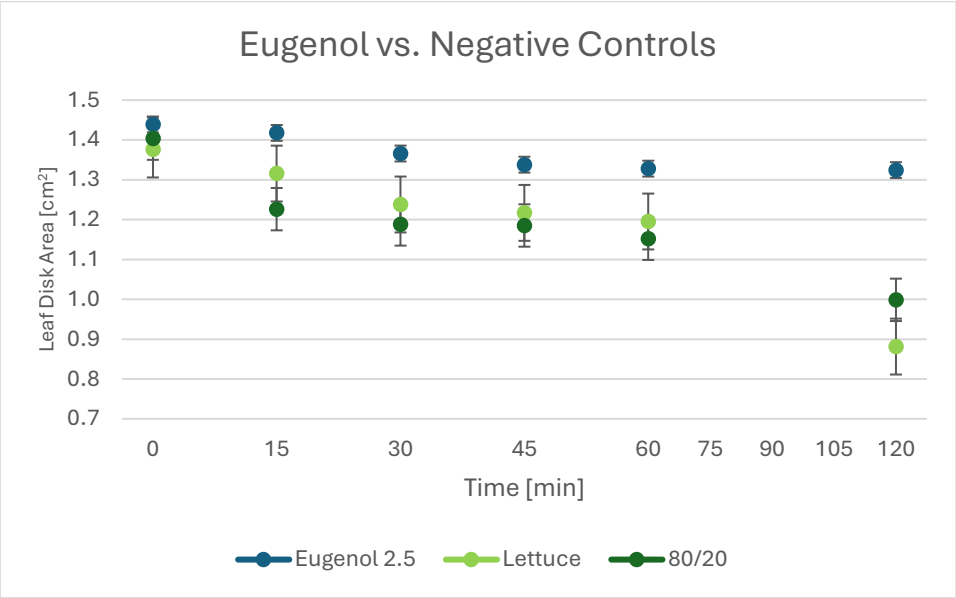

Figure 13: Comparison of the remaining areas of leaf disks after feeding by *S. littoralis* over a period of 120 minutes. One set of leaf disks contained eugenol (at a concentration of 2.5 mg/mL) while the others provided negative controls: a plain lettuce control with no additional solution and a control with the negative control (80:20 water/acetone solution).

Figure 14 depicts the impacts of the eugenol stock compound at different concentrations on the feeding rate of *S. littoralis*. Although the 2.5 mg/mL solution predictably slows the feeding rate the most, the 0.625 mg/mL shows a similar reduction. Surprisingly, the 1.25 mg/mL seems to have the least deterrent effect when compared to the other two concentrations. This trend was also found in comparisons of differing concentrations of hydroxychavicol (**1**), and 2-methoxy-4-(2-propen-1-yl)phenyl-6-*O*-D-apio-β-D-furanosyl-β-D-glucopyranoside (**2**). In other words, in all eugenol derivative compounds, the concentration of 0.625 mg/mL was found similarly effective, if not more effective, at reducing feeding activity.

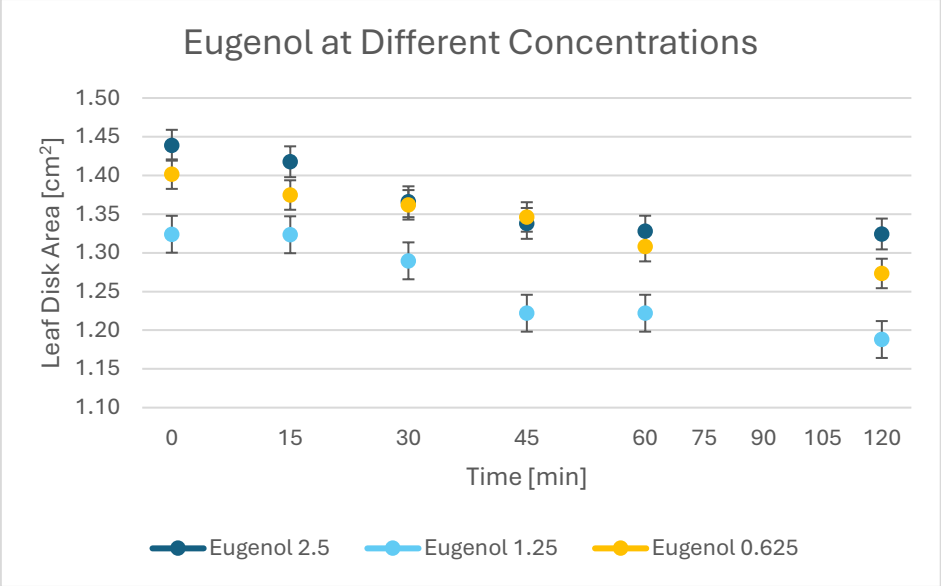

Figure 14: Comparison of the remaining areas of leaf disks after feeding by *S. littoralis* over a period of 120 minutes. Leaf disks were distributed with 2.5, 1.25, and 0.625 mg/mL of eugenol stock solution.

Because concentrations of 0.625 mg/mL were determined similarly effective at reducing herbivory when compared to 2.5 mg/mL, and because lower concentrations are likely more reflective of the production rate of eugenol compounds in *F. tamberlikiana*, lower concentrations were used for the final comparison. Here, it should be noted that all eugenol derivative compounds are as effective, if not more effective when compared to caffeine, which is set to a concentration of 2.5 mg/mL. All three eugenol compounds show a reduction in feeding activity when compared to the 80:20 water/acetone control, with 2-methoxy-4-(2-propen-1-yl)phenyl-6-*O*-D-apio-β-D-furanosyl-β-D-glucopyranoside (**2**) (Figure 15; noted on the graph as NMR05) performing slightly better than all other compounds. This compound is non-volatile and therefore its deterrent effect may occur after oral uptake.

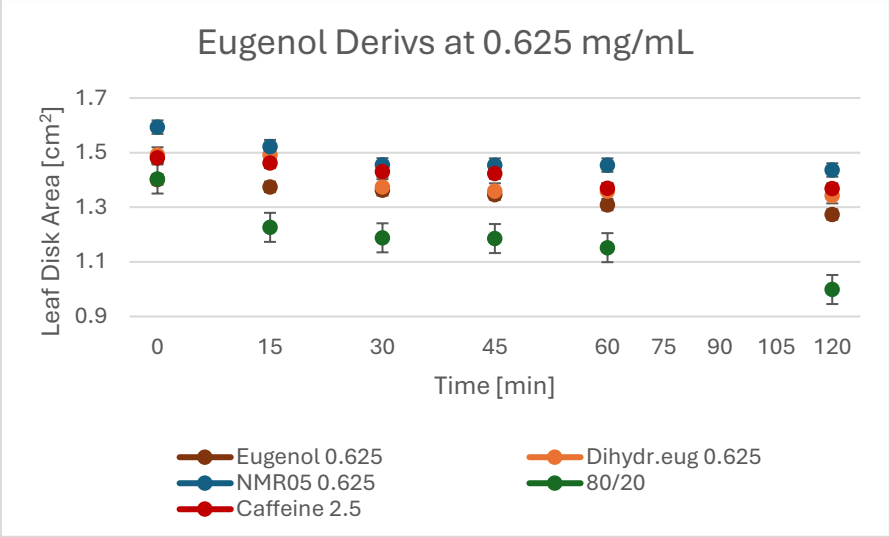

Figure 15: Comparison of the remaining areas of leaf disks after feeding by *S. littoralis* over a period of 120 minutes. All eugenol derivatives were set to a concentration of 0.625 mg/mL, caffeine (positive control) and the 80:20 water/acetone (= negative control) were provided as controls

When eugenol was compared at different concentrations (2.5, 1.25, and 0.625 mg/mL), it was shown that the 2.5 and 0.625 mg/mL solutions perform similarly well at reducing herbivory, while 1.25 mg/mL reduces feeding by a lower margin. This trend was found to be true of both eugenol derivatives extracted from *F. tamberlikiana*: hydroxychavicol (**1**), and 2-methoxy-4-(2-propen-1-yl)phenyl-6-*O*-D-apio-β-D-furanosyl-β-D-glucopyranoside (**2**). Even at these low concentrations, all three compounds reduced feeding activity compared to 80:20 lettuce and similarly well to caffeine. From this information, it can be inferred that *F. tamberlikiana* produces these compounds in leaf tissues as a defense against herbivory.

Additional studies would be needed to assess the effect of eugenol and its derivatives on the lifetime fitness of these insects to determine whether they impact lifespan and reproductive capabilities and whether these compounds can be considered truly insecticidal. One aspect that this study was unable to analyze but was visually apparent was that all eugenol compounds induced some degree of vomiting in *S. littoralis*, suggesting they could impart serious harm to herbivores. However, it was outside of the scope of the data to assess how much or how often regurgitation occurred. This study also lacks information about whether *S. littoralis* (and therefore other generalists) can build up a tolerance to these compounds over time and how quickly this can happen, perhaps with repeated exposure these compounds are not as harmful

as they appear upon first glance. More information is certainly needed to shed light on the role these compounds play in complex ecosystems, both within *Faramea tamberlikiana* and the genus as a whole.

4.0 Conclusion

This study represents the first investigation into the phytochemical profile of *Faramea tamberlikiana* and is one of only eight published studies on the phytochemistry of the genus as a whole. Seven key compounds were isolated and identified: hydroxychavicol (**1**), the two eugenol derivatives 2-methoxy-4-(2-propen-1-yl)phenyl-6-*O*-D-apio-β-D-furanosyl-β-D-glucopyranoside (**2**) and ligusinenoside A (**3**), blumenol C glucoside (**4**), deacetylasperulosidic acid (**5**), tectoridin (**6**), and vanillic acid (**7**), thereby enhancing our understanding *Faramea tamberlikiana*'s phytochemical profile. These compounds are derived from four different biosynthetic pathways: the phenylpropanoid- (**1**, **2**, **3**), terpenoid- (**4**, **5**), flavonoid- (**6**), and benzoic acid pathway (**7**).

While existing literature shows that the genus *Faramea* primarily accumulates phenylpropanoids and iridoids (Table 1), this study reveals that in *F. tamberlikiana*, iridoids play a only minor role, while phenylpropanoids, namely eugenol derivatives, dominate the phytochemical landscape (Figure 11). This represents a slight divergence from the broader genus profile. Further research may support the notion that phenylpropanoids serve as important chemotaxonomic markers within the *Faramea* genus, with iridoids acting as secondary markers. Interestingly, the *Rubiaceae* family is more commonly recognized for the prevalence of alkaloids, which have not yet been isolated in *Faramea*, thereby distinguishing this genus within the family. Additionally, no eugenol derivatives have been identified in other members of the *Rubiaceae* family to date. These observations underscore the significance of chemotaxonomy in understanding the unique chemical ecology and classification of *Faramea*.

The insect assay conducted in this study provides further insight into the ecological role of the compounds present in *F. tamberlikiana*. One of the compounds isolated directly from *F. tamberlikiana* dried leaf material, 2-methoxy-4-(2-propen-1-yl)phenyl-6-*O*-D-apio-β-D-furanosyl-β-D-glucopyranoside (**2**), was more effective

than any of the control compounds (caffeine, salicin, and aristolochic acid) in reducing the area of leaf disks consumed by the larvae. This demonstrates a direct connection between the plant's compounds and their deterrent effects on herbivory, which provides evidence that these abundant phenylpropanoids contribute to protection against insect pests.

The defensive mechanism seen in *F. tamberlikiana* may be similar to that of the "mustard oil bomb" system found in plants that produce glucosinolates. In these systems, glucosinolates are hydrolyzed into bitter, toxic compounds when plant tissues are damaged, deterring herbivory. Similarly, the phenylpropanoid glycosides in *F. tamberlikiana* may act as a chemical defense, particularly in leaf tissues, by release of volatile eugenol, thus discouraging herbivores like *S. littoralis*. This suggests an evolved defensive strategy that parallels the mustard oil bomb mechanism, where compounds are stored in a stable form in the vacuole and activated upon herbivore interaction.

Given that the *Faramea* genus remains understudied, further research is necessary to delve deeper into the phytochemistry of this taxon. Future studies should explore phytochemistry of additional genus members, as relatively few have been studied. In much the same way that chemotaxonomic studies have helped shed light on the complex and interwoven evolutionary history of the *Psychotrieae* alliance, similar techniques should be considered for the *Coussareeae* tribe and its major clades. Given its characteristic heterogeneous morphology and the need for DNA analysis to clarify taxonomic relationships, additional compound analysis may help to strengthen evidence of shared ancestry or a necessity for reclassification. As of yet, there are no studies that link the phylogeny of *Coussareeae*, or *Faramea* specifically, with its major phytochemical constituents.

5.0 References

Barboza, R.S., Valente, L.M.M., Wolff, T., Assunção-Miranda, I., Neris, R.L.S., Guimarães-Andrade, I.P., Gomes, M. 2018. Antiviral Activity of *Faramea hyacinthina* and *Faramea truncata* Leaves on Dengue Virus Type-2 and their Major Compounds. *Chemistry and Biodiversity,* 15 (2): Epub. https://doi.org/10.1002/cbdv.201700393.

Baskar, K., Sasikumar, S., Muthu, C., Kingsley, S., Ignacimuthu, S., 2011. Bioefficacy of *Aristolochia tagala* Cham. against *Spodoptera litura* Fab. (Lepidoptera: Noctuidae). *Saudi Journal of Biological Sciences*, 18(1):23–27. https://doi.org/10.1016/j.sjbs.2010.09.004.

Berger, A., Preinfalk, A., Robien, W., Brecker, L., Valant-Vetschera, K., Schinnerl, J. 2016. New reports on flavonoids, benzoic- and chlorogenic acids as rare features in the *Psychotria* alliance (*Rubiaceae*). *Biochemical Systematics and Ecology,* 66: 145–153. https://doi.org/10.1016/j.bse.2016.02.027.

Berger, A., Kostyan M., Klose S., Gastegger M., Lorbeer E., Brecker L., Schinnerl J. 2015. Loganin and secologanin derived tryptamine–iridoid alkaloids from *Palicourea crocea* and *Palicourea padifolia* (*Rubiaceae*). *Phytochemistry*, 116:162–169. https://doi.org/10.1016/j.phytochem.2015.05.013.

Berger, A., Valant-Vetschera, K., Schinnerl, J. 2021. A revised classification of the sister tribes *Palicoureeae* and *Psychotrieae* (*Rubiaceae*) indicates genus-specific alkaloid accumulation. *Phytochemistry Reviews,* 21: 941–986. https://doi.org/10.1007/s11101-021-09769-x.

Berger, A., Vetschera, K., Schinnerl, J., Brecker, L. 2022. Alkaloid Diversification in the Genus *Palicourea* (*Rubiaceae: Palicoureeae*) Viewed from a (Retro-) biogenetic Perspective. *Phytochemistry Reviews*, 21: 941–986. https://doi.org/10.1007/s11101-021-09768-y.

Bremer, B., Andreasen, K., Olsson, D. 1995. Subfamilial and Tribal Relationships in the *Rubiaceae* Based on rbcL Sequence Data. *Annals of the Missouri Botanical Garden,* 82: 383–397. https://doi.org/10.2307/2399889.

Bremer, B., Eriksson, T. 2009. Time Tree of *Rubiaceae*: Phylogeny and Dating the Family, Subfamilies, and Tribes. *International Journal of Plant Sciences*, *170*(6): 766–793. https://doi.org/10.1086/599077.

Cherney, E., Baran, P. 2011. Terpenoid-Alkaloids: Their Biosynthetic Twist of Fate and Total Synthesis. *Israel Journal of Chemistry*, 51(3-4): 391–405. https://doi.org/10.1002/ijch.201100005.

Cheng, W., Fang, X., Guan, Z., Yao, Y., Xu, Z., Bi, Y., Ren, K., Li, J., Chen, F., Chen, X., Ma, W., Chu, Z., Deng, Z., Zhang, Z., Lu, L. 2023. Functional characterization and structural basis of a reversible glycosyltransferase involves in plant chemical defence. *Plant Biotechnology Journal,* 21(12): 2611–2624. https://doi.org/10.1111/pbi.14157.

Commonwealth Agricultural Bureaux International (CABI). 2022. *Spodoptera littoralis* (cotton leafworm). *Plantwise Knowledge Bank*. https://plantwiseplusknowledgebank.org/doi/full/10.1079/pwkb.species.20937. Accessed: 30 June 2024.

Ferrari, F., Delle Monache, G., Alves de Lima, R. 1985. Two Naphthopyran Derivatives from *Faramea cyanea*. *Phytochemistry,* 24(11): 2753–2755. https://doi.org/10.1016/S0031-9422(00)80719-0.

Glendinning, J.I., Davis, A., Ramaswamy, S. 2002. Contribution of Different Taste Cells and Signalling Pathways to the Discrimination of "Bitter" Taste Stimuli by an Insect. *The Journal of Neuroscience*, 22(16): 7281–7287. https://doi.org/10.1523/JNEUROSCI.22-16-07281.2002.

Govaerts, R. 2017. World Checklist of Selected Plant Families. In O. Bánki, Y. Roskov, L. Vandepitte, R. E. DeWalt, D. Remsen, P. Schalk, T. Orrell, M. Keping, J. Miller, R. Aalbu, R. Adlard, E. Adriaenssens, C. Aedo, E. Aescht, N. Akkari, M. A. Alonso-

Zarazaga, B. Alvarez, F. Alvarez, G. Anderson, Catalogue of Life Checklist (Version 2021-08-25). *Catalogue of Life*. https://doi.org/10.48580/d4sd-38c.

Hosseini Mousavi, S.M., Hemmati, S.A., Rasekh, A. 2023. Feeding responses and digestive function of *Spodoptera littoralis* (Boisduval) on various leafy vegetables exhibit possible tolerance traits. *Bulletin of Entomological Research*, 113(3):430–438. https://doi.org/10.1017/S000748532300010X.

Hou, X., Rivers, J., León, P., McQuinn, R., Pogson, B. 2016. Synthesis and Function of Apocarotenoid Signals in Plants. *Trends in Plant Science*, 21(9): 792–803. https://doi.org/10.1016/j.tplants.2016.06.001.

Hussein, H.S., Salem, M.Z.M., Soliman, A.M. 2023. Comparative Study of Three Plant-Derived Extracts as New Management Strategies Against *Spodoptera littoralis* (Boisduval) (*Lepidoptera: Noctuidae*). *Scientific Reports*, 13: 3542. https://doi.org/10.1038/s41598-023-30588-x.

Koeduka, T., Fridman, E., Gang, D., Vassão, D., Jackson, B., Kish, C., Orlova, I., Spassova, S., Lewis, N., Noel, J., Baiga, T., Dudareva, N., Pichersky, E. 2006. Eugenol and isoeugenol, characteristic aromatic constituents of spices, are biosynthesized via reduction of a coniferyl alcohol ester. *Proceedings of the National Academy of Sciences* (PNAS), 103(26): 10128–10133. https://doi.org/10.1073/pnas.0603732103.

Kornpointner, C., Hochenegger, N., Shi, B., Berger, A., Theiner, J., Brecker L, Schinnerl, J. 2022. Phytochemistry meets Geochemistry—Blumenol C sulfate: A new megastigmane sulfate from *Palicourea luxurians* (*Rubiaceae: Palicoureeae*). *Molecules*, 27: 7284. https://doi.org/10.3390/molecules27217284.

Liao, P., Hemmerlin, A., Bach, T.J., & Chye, M. 2016. The potential of the mevalonate pathway for enhanced isoprenoid production. *Biotechnology Advances,* 34(5): 697–713. https://doi.org/10.1016/j.biotechadv.2016.03.005.

Liu W., Feng Y., Yu S., Fan Z., Li X., Li J., Yin H. 2021 The Flavonoid Biosynthesis Network in Plants. *International Journal of Molecular Sciences*, 22(23): 12824. https://doi.org/10.3390/ijms222312824.

Löfstrand, S.D., Razafimandimbison, S.G., Rydin, C. 2019. Phylogeny of Coussareeae (*Rubioideae*, *Rubiaceae*). *Plant Systematics and Evolution,* 305, 293–304. https://doi.org/10.1007/s00606-019-01572-8.

Löfstrand, S.D., Taylor, C.M., Razafimandimbison, S.G., Rydin, C. 2021. Phylogenetic Relationships, Infrageneric Classification and Species Limits in the Neotropical Genus *Faramea* (*Coussareeae*: *Rubiaceae*), *Botanical Journal of the Linnean Society*, 197(4): 478–497, https://doi.org/10.1093/botlinnean/boab034.

Lu, Q., Wang, J., Kong, L. 2014. Chemical constituents from *Psychotria yunnanensis* and its chemotaxonomic study *Biochemical Systematics & Ecology,* 52: 20–22. https://doi.org/10.1016/j.bse.2013.11.002.

Ma, J., & Tan, C.H., Zhu, D.Y. 2007. Chemical constituents of *Ligusticum sinensis* OLIV. *Helvetica Chimica Acta*, 90: 158–163. https://doi.org/10.1002/hlca.200790010.

Martins, D., Nunez, C.V. 2015 Secondary Metabolites from *Rubiaceae* Species. *Molecules*, 20(7): 13422–13495. https://doi.org/10.3390/molecules200713422.

Metsämuuronen, S., Sirén, H. 2019. Bioactive phenolic compounds, metabolism and properties: a review on valuable chemical compounds in Scots pine and Norway spruce. *Phytochemistry Reviews*, 18: 623–664. https://doi.org/10.1007/s11101-019-09630-2.

Miettinen, K., Dong, L., Navrot, N. 2014. The seco-iridoid pathway from *Catharanthus roseus*. *Nature Communications*, 5: 3606. https://doi.org/10.1038/ncomms4606.

Mitova, M., Anchev, M., Handjieva, N., Popov, S. 2002. Iridoid Patterns in *Galium* L. and Some Phylogenetic Considerations. *Zeitschrift für Naturforschung C*, 57(3-4): 226–234. https://doi.org/10.1515/znc-2002-3-405.

Mongrand, S., Badoc, A., Patouille, B., Lacomblez, C., Chavent, M., Bessoule, J., 2005. Chemotaxonomy of the *Rubiaceae* family based on leaf fatty acid composition, *Phytochemistry*, 66(5): 549–559. https://doi.org/10.1016/j.phytochem.2004.12.021.

Nállarett, D. 2024. *Faramea tamberlikiana Müll. Arg. Rubiaceae*. Field Museum of Natural History. https://plantidtools.fieldmuseum.org/en/nlp/catalogue/3362914.

Naoumkina, M., Zhao, Q., Gallego-Giraldo, L., Dai, X., Zhao, P., Dixon, R. 2010. Genome-wide analysis of phenylpropanoid defence pathways. *Molecular Plant Pathology*, 11(6):829-46. https://10.1111/j.1364-3703.2010.00648.x.

Nascimento, A. C., Valente, L. M. M., Gomes, M., Barboza, R. S., Wolff, T., Neris, R. L. S., Figueiredo, C. M., & Assunção-Miranda, I. 2017. Antiviral activity of *Faramea bahiensis* leaves on dengue virus type-2 and characterization of a new antiviral flavanone glycoside. *Phytochemistry Letters*, 19: 220–225. https://doi.org/10.1016/j.phytol.2017.01.013.

O'Connor, S.E., Maresh, J.J., 2006. Chemistry and biology of monoterpene indole alkaloid biosynthesis. *Natural Product Reports*, 23: 532–547. https://doi.org/10.1039/b512615k.

Oldřich Lapčík. 2007. Isoflavonoids in non-leguminous taxa: A rarity or a rule? *Phytochemistry*, 68(22–24): 2909–2916. https://doi.org/10.1016/j.phytochem.2007.08.006.

Osa Conservation Campus. 2022, April 25. *Faramea tamberlikiana*. Osa Arboretum. https://osa-arboretum.org/plant/faramea-tamberlikiana/.

Pott, D., Osorio, S., Vallarino, J., 2019. From Central to Specialized Metabolism: An Overview of Some Secondary Compounds Derived From the Primary Metabolism for Their Role in Conferring Nutritional and Organoleptic Characteristics to Fruit. *Frontiers in Plant Science*, 28(10): 835. https://doi.org/10.3389/fpls.2019.00835.

Robbrecht, E. Manen, J. 2006. The Major Evolutionary Lineages of the Coffee Family (*Rubiaceae*, Angiosperms). Combined Analysis (nDNA and cpDNA) to Infer the Position of *Coptosapelta* and *Luculia*, and Supertree Construction Based on rbcL, rps16, trnL-trnF and atpB-rbcL Data. A New Classification in Two Subfamilies, *Cinchonoideae* and *Rubioideae*. *Systematics and Geography of Plants*, 76: 85–146.

Rocha-Filho, L., Garófalo, C. 2013. Community ecology of euglossine bees in the coastal Atlantic Forest of São Paulo State, Brazil, *Journal of Insect Science*, (13)1: 23. https://doi.org/10.1673/031.013.2301.

Ross, S., Zagloul, A., Nimrod, A., Mehmedic, Z., & Elsohlyl, H. 1999. A Cytotoxic Chalcone from *Faramea salicifolia*. *Planta Medica*, 65(2): 194. https://doi.org/10.1055/s-2006-960468.

Sauvain, M., Dedet, J.-P., Kunesch, N., Poisson, J. 1994. Isolation of Flavans from the Amazonian Shrub *Faramea guianensis*. *Journal of Natural Products*, 57(3): 403–406. https://doi.org/10.1021/np50105a014.

Schinnerl, J., Orlowska, E., Lorbeer, E., Berger, A., Brecker, L. 2012. Alstrostines in *Rubiaceae*: Alstrostine A from *Chassalia curviflora* var. *ophioxyloides* and a novel derivative, rudgeifoline from *Rudgea cornifolia*. *Phytochemistry Letters*, 5(3): 586–590. https://doi.org/10.1016/j.phytol.2012.05.019.

Schmid, J., Amrhein, N. 1995. Molecular organization of the shikimate pathway in higher plants. *Phytochemistry*, 39(4), 737–749. https://doi.org/10.1016/0031-9422(94)00962-S.

Seada, M.A., Ignell, R., Al Assiuty, A.N., Anderson, P. 2018. Functional Characterization of the Gustatory Sensilla of Tarsi of the Female Polyphagous Moth *Spodoptera littoralis*. *Front Physiology,* 14(9): 1606. https://doi.org/10.3389/fphys.2018.01606.

Seigler, D.S. 1998. Iridoid Monoterpenes. *Plant Secondary Metabolism*. Springer, Boston, MA. https://doi.org/10.1007/978-1-4615-4913-0_20.

Sherden, N., Lichman, B., Caputi, L., Zhao, D., Kamileen, M., Buell, C. O'Connor, S. 2017. Identification of Iridoid Synthases from *Nepeta* Species: Iridoid Cyclization Does Not Determine Nepetalactone Stereochemistry. *Phytochemistry,* 145: 48–56. https://doi.org/10.1016/j.phytochem.2017.10.004.

Stevens, P.F. Angiosperm Phylogeny Website. Version 14, July 2017. http://www.mobot.org/MOBOT/research/APweb/.

Tan, K., Nishida, R. 2012. Methyl Eugenol: Its Occurrence, Distribution, and Role in Nature, Especially in Relation to Insect Behavior and Pollination. *Journal of Insect Science* 12(1): 56. http://doi.org/10.1673/031.012.5601.

Taiz, L., Zeiger, E. 2002. *Plant Physiology*. Sunderland, Massachusettes: Sinauer Associates.

Taylor, C.M., Jardim, J.G. 2020. Rubiacearum Americanarum Maga Hama Pars XLVI: New Species and Taxonomic Changes in *Faramea* of Central and South America (*Coussareeae*). *Novon,* 28: 108–142. http://doi.org/10.3417/2019552.

Thureborn, O., Razafimandimbison, S., Wikström, N., Rydin, C. 2022. Target Capture Data Resolve Recalcitrant Relationships in the Coffee Family (*Rubioideae, Rubiaceae*). *Front Plant Science*, 13: 967456. http://doi.org/10.3389/fpls.2022.967456.

Tissier, A., Ziegler, J., Vogt, T. 2014. Specialized Plant Metabolites: Diversity and Biosynthesis. *Ecological Biochemistry*, 2: 14–32. https://doi.org/10.1002/9783527686063.ch2.

Tzin, V., Galili, G. 2010. New Insights into the Shikimate and Aromatic Amino Acids Biosynthesis Pathways in Plants. *Molecular Plant* 3: 956–972. http://doi.org/10.1093/mp/ssq048.

Vogt, T. 2010. Phenylpropanoid biosynthesis. *Molecular Plant* 3(1): 2–20. http://doi.org/10.1093/mp/ssp106.

Wang, M., Schäfer, M., Li, D., Halitschke, R., Dong, C., McGale, E., Paetz, C., Song, Y., Li, S., Dong, J., Heiling, S., Groten, K., Franken, P., Bitterlich, M., Harrison, M.J., Paszkowski U., Baldwin I.T. 2018. Blumenols as shoot markers of root symbiosis with arbuscular mycorrhizal fungi. *Elife*, 28(7): e37093. http://doi.org/10.7554/eLife.37093.

Wolff, T., Valente, L.M.M., Barboza, R.S., Berrueta, L.A., Gallo, B., Gomes, M. 2019. Iridoid Glucosides from the Stems of Three Bioactive Brazilian *Faramea* species (*Rubiaceae*). *Biochemical Systematics and Ecology*, 84: 35–36. https://doi.org/10.1016/j.bse.2019.03.009.

Wolff, T., Berrueta, L., Valente, L., Barboza, R., Neris, R., Guimarães-Andrade, I., Assunção-Miranda, I., Nascimento, A., Gomes, M., Gallo, B., Iriondo, C. 2018. Comprehensive characterisation of polyphenols in leaves and stems of three anti-dengue virus type-2 active Brazilian *Faramea* species (*Rubiaceae*) by HPLC-DAD-ESI-MS/MS. *Phytochemical Analysis*, 30(1): 62–72. https://doi.org/10.1002/pca.2790.